A comparison of landslide inventories along the shoreline of Steamboat Island Peninsula, Thurston County, WA: office based protocol vs. field based protocol

Dorothy M. Metcalf-Lindenburger

A report prepared in partial fulfillment of

the requirements for the degree of

Master of Science

Earth and Space Sciences: Applied Geosciences

University of Washington

June, 2016

Project mentor:

Daniel J. Miller

Internship coordinator:

Kathy G. Troost

Reading committee:

Alison Duvall

Steven Walters

MESSAGe Technical Report Number: 033

Executive Summary

The mountain ranges and coastlines of Washington State have steep slopes, and they are susceptible to landslides triggered by intense rainstorms, rapid snow melts, earthquakes, and rivers and waves removing slope stability. Over a 30-year timespan (1984-2014 and includes State Route (SR) 530), a total of 28 deep-seated landslides caused 300 million dollars of damage and 45 deaths (DGER, 2015). During that same timeframe, ten storm events triggered shallow landslides and debris flows across the state, resulting in nine deaths (DGER, 2015). The loss of 43 people, due to the SR 530 complex reactivating and moving at a rate and distance unexpected to residents, highlighted the need for an inventory of the state's landslides. With only 13% of the state mapped (Lombardo et al., 2015), the intention of this statewide inventory is to communicate hazards to citizens and decision makers.

In order to compile an accurate and consistent landslide inventory, Washington needs to adopt a graphic information system (GIS) based mapping protocol. A mapping protocol provides consistency for measuring and recording information about landslides, including such information as the type of landslide, the material involved, and the size of the movement. The state of Oregon shares similar landslide problems as Washington, and it created a GIS-based mapping protocol designed to inform its residents, while also saving money and reducing costly hours in the field (Burns and Madin, 2009). In order to determine if the Oregon Department of Geology and Mineral Industries (DOGAMI) protocol, developed by Burns and Madin (2009), could serve as the basis for establishing Washington's protocol, I used the office-based DOGAMI protocol to map landslides along a 40-50 km (25-30 mile) shoreline in Thurston County, Washington. I then compared my results to the field-based landslide inventory created in 2009 by the Washington Division of Geology and Earth Resources (DGER) along this same shoreline. If the landslide area I mapped reasonably equaled the area of the DGER (2009) inventory, I would consider the DOGAMI protocol useful for Washington, too.

Utilizing 1m resolution lidar flown for Thurston County in 2011 and a GIS platform, I mapped 36 landslide deposits and scarp flanks, covering a total area of 879,530 m^2 (9,467,160 ft^2). I also found 48 recent events within these deposits. With an exception of two slides, all of the movements occurred within the last fifty years. Along this same coastline, the DGER (2009) recorded 159 individual landslides and complexes, for a total area of 3,256,570 m^2 (35,053,400 ft^2). At a first glance it appears the DGER (2009) effort found a larger total number and total area of landslides. However, in addition to their field inventory, they digitized landslides previously mapped by other researchers, and they did not field confirm these landslides, which cover a total area of 2,093,860 m^2 (22,538,150 ft^2) (DGER, 2009). With this questionable landslide area removed and the toes and underwater landslides accounted for

because I did not have a bathymetry dataset, my results are within 6,580 m^2 (70,840 ft^2) of the DGER's results.

This similarity shows that the DOGAMI protocol provides a consistent and accurate approach to creating a landslide inventory. With a few additional modifications, I recommend that Washington State adopts the DOGAMI protocol. Acquiring additional 1m lidar and adopting a modified DOGAMI protocol poises the DGER to map the remaining 87% of the state, with an ultimate goal of informing citizens and decision makers of the locations and frequencies of landslide hazards on a user-friendly GIS platform.

Table of Contents

List of Figures

List of Tables

Acknowledgements

The danger of writing down whom I want to thank, is that I will leave someone critical out. However, it seems equally rude to assume I accomplished this research alone, when this has really been an effort supported by many talented and gracious people. Therefore, I would like to thank:

- Alison Duvall, Dan Miller, and Steven Walters—my reading committee and mentors;
- William (Bill) Burns, from Oregon Department of Geology and Mineral Industries (DOGAMI), for meeting with me about the protocol he helped write and answering follow up phone calls and emails;
- The Washington Division of Geology and Earth Resources (DGER), including Dave Norman, Tim Walsh, Stephen Slaughter, and especially, Michael Polenz, the principal investigator on the shoreline landslides of Thurston County, WA, who gave me armloads and computer files of data;
- Owen Reynolds from Thurston County GeoData for meeting and providing answers about the 2011 lidar;
- Mark Biever from Thurston County Water Resources also spent an afternoon giving me details about the Sunrise and Carlyon/Hunter Point Landslides, and then he drove with me out to both spots to conduct brief field observations;
- Wendy Gerstel for answering initial questions and providing research ideas;
- The University of Washington professors involved in MESSAGe, especially Juliet Crider and Kathy Troost for providing support and guidance;
- Connor Kee, peer editor;
- My husband and daughter, for their unconditional support.

Introduction

On March 22, 2014, at 1037 PDT, a landslide that transitioned into a debris flow covered the Steelhead Haven neighborhood in Washington State on State Route (SR) 530 (Keaton et al., 2014). The landslide killed 43 people, buried over 40 homes, and caused over 80 million dollars of damages (Keaton et al., 2014; Lombardo et al., 2015; DGER, 2015). In the three decades prior to this event, landslide events, triggered by intense rainstorms, rapid snow melts, earthquakes, and rivers and waves removing slope stability, killed eleven others and caused approximately $220 million dollars of damage (DGER, 2015). Despite all of this destruction, the state currently lacks a landslide mapping protocol (Slaughter, 2015). The severity of the SR 530 landslide resulted in the governor forming an independent commission; this SR 530 Commission recommended a "statewide landslide hazard risk mapping program" (Lombardo et al., 2015).

The state needs this program because land-use planners, decision makers, and community members—both urban and rural—require access to information regarding geological hazards. Few of the past efforts for mapping these hazards are at a scale that home or business owners can recognize their property. Current and future efforts require a level of detail found at the scale of 1:24,000 (1in = 2,000ft) or larger. Additionally, geologists using graphic information systems (GIS) with 1-2m lidar data are able to identify more hazards and show the extent of these hazards accurately (Haugerud et al., 2003; Schulz, 2007; McKenna et al., 2008). Currently, only 13% of the Washington State is geologically mapped at the scale of 1:24,000 (Lombardo et al., 2015), and only 25%-35% of the state has lidar coverage, with a significant portion of this data considered questionable, according to the Washington State Department of Natural Resources (http://www.dnr.wa.gov/lidar#current-projects.1).

Other states with steep slopes have prioritized increased hazard mapping efforts. For example, Oregon uses extensive lidar and GIS platforms to map landslide hazards. As of 2015, Oregon had 33.5% of the state covered by high-resolution lidar (eight pulses per square meter) (Ryan, 2015). This is due to the efforts of Burns and Madin (2009) and the creation of their landslide mapping protocol established for the Oregon Department of Geology and Mineral Industries (DOGAMI). Their protocol requires mapping landslides on a GIS system, and layering DEM derived from lidar data with orthorectified aerial photos and geologic maps. In the same year, Washington Division of Geology and Earth Resources (DGER) released the results of its landslide survey along the marine shore of Thurston County (DGER, 2009). Both teams used GIS with lidar data to record the extent of the landslides. Additionally, Oregon established their protocol as the basis for their statewide landslide information database for Oregon (SLIDO).

A statewide protocol and landslide inventory will not prevent landslide hazards. However, at the very least it can inform individual decision makers on how to select and protect property, and at its greatest it can inform the decisions of local governments and leaders. Additionally, a statewide inventory can lead to better probability and slope stability modeling and warnings so that these hazards do not become disasters.

This study focuses on testing the office-based DOGAMI protocol against the field-based protocol used by the DGER (2009). Unable to map the entire shoreline of Thurston County, WA, I limited my study area to Steamboat Island Peninsula north of Highway 101 (Figure 1). Specifically, I hypothesize that I can use the DOGAMI protocol to identify landslides along the shoreline of Steamboat Island Peninsula, using GIS and 1m-resolution lidar, and that the landslide area I map will be similar to the area mapped by the DGER. Assuming these areas are similar, indicating the DOGAMI protocol is acceptable for using as a basis for Washington's protocol, I will assess the strengths and weaknesses of both approaches and provide recommendations for future statewide adoption.

Geographic and Geologic Setting

The landslides along the shoreline of Steamboat Island Peninsula are a result of the interaction of water, people, and geology.

Geography and Brief History

Steamboat Island Peninsula is located at the southern tip of Puget Sound on the western edge of Thurston County, WA. The highest point on the peninsula is just over 80m (260ft) and found north of Schneider Creek. The drainages along the peninsula are short, and they direct water away from a divide that hugs the northwestern shoreline. A majority of the peninsula shoreline drops steeply from 40-45m (130-150ft) down to sea level. Along the western shoreline, the drift cell movement is left to right, and along the eastern shoreline, it is right to left (https://fortress.wa.gov/ecy/coastalatlas/tools/Map.aspx).

Humans have altered the geography of the peninsula, redirecting water flow, removing root strength provided by trees, and creating roads and neighborhoods along steep bluffs. While Native Americans lived in the vicinity for thousands of years, the arrival of Euro-Americans changed the landscape significantly (Thurston County Development Services Department, 2008). Logging in the county began in 1889, but exactly when it reached Steamboat Island Peninsula is unclear. Aerial photos show increased clearings beginning in 1965. After the 1970s, residents built homes and neighborhoods. Clearing obstructions for views of the water and mountains, several landowners removed trees and constructed their homes right near the edge of the steep shoreline bluffs.

Geology

As part of the Puget Sound, Steamboat Island Peninsula is located in a physiographic basin known as the Puget Lowland, which extends from northeast of Vancouver Island, Canada southeastward towards southern Washington (Booth, 1987; Troost and Booth, 2008) (Inset map of Figure 2). The Olympic Mountains establish the western boundary of this basin, and the Cascade Mountains define the eastern boundary (Figure 2). While hard rock exists within the study area, the majority of the peninsula is made up of glacial sediments. The landslides occur within these sediments. Furthermore, tectonic activity and recent faulting add additional instability to the area.

The oldest rocks in the mapping region crop out just south of Steamboat Island Peninsula in the Black Hills (Figure 3). The Black Hills are made up of Lower Eocene volcanics, known as the Crescent Formation. These basaltic breccias, sills, dikes, and flows are thought to be the result of rifting between the Kula and Farallon plates as they converged obliquely with the North American Plate (Duncan, 1982; Logan and Walsh, 2004). Around 48-36 million years ago, spreading and subduction dynamics shifted, and the Juan de Fuca Plate began subduction beneath the North American Plate (Duncan, 1982; Pratt et al., 1997). These rocks of the Black Hills disappear steeply beneath Steamboat Island Peninsula, and this abrupt change, known as the Olympia Structure, is interpreted as either a monocline or part of a "thin-skinned" thrust sheet (Pratt et al., 1997; Logan and Walsh, 2004; Clement et al., 2010) (Figure 3). Above the Crescent Formation are possibly younger Eocene or Oligocene sediments, which are all overlain by Quaternary sediments (Booth, 1987, 1994; Pratt et al., 1997; Logan and Walsh, 2004; Troost and Booth, 2008).

The Puget Lowland provided the structural trough for the advancement and retreats of the Puget Lobe of the Cordilleran ice sheet (Booth, 1987, 1994; Troost and Booth, 2008) (Figure 2). Each advancement and retreat of the Puget Lobe reworked and buried prior sediments, and not all ice advancements reached Thurston County (Booth, 1987, 1994; Logan et al., 2003). Steamboat Island Peninsula has sediments that are pre-Vashon in age and deposited both from ice and from local rivers (Logan et al., 2003; Schasse et al., 2003; Walsh et al., 2003; Logan and Walsh, 2004) (Table 1). The most recent advancement of the Puget Lobe, known as the Vashon stade of the Fraser glaciation, reached its furthest extent into the Black Hills after ^{14}C 13,430 years B.P. (Booth, 1987, 1994; Borden and Troost, 2001; Logan and Walsh, 2004) (Figures 2). It created a proglacial lake that filled with fine grained sediment and then with coarser sands (Booth, 1987, 1994; Troost and Booth, 2008). Eventually, ice covered the southern Puget Lowland to a depth of about 300m (1,000ft) (Booth, 1987). Water flowing beneath the ice created large features, including the divisions between Steamboat Island Peninsula and the other three peninsulas of Thurston County (Booth, 1994).

The exact timing of the retreat of the ice sheet from this study area is unclear (Booth, 1997; Borden and Troost, 2001). As it retreated, a large lake—Glacial Lake Russell—formed; the lowest point of the Black Hills controlled its depth, with spills going south into the Chehalis River (Troost and Booth, 2008) (Figure 2). Recessional outwash followed by recessional fines filled this body of water, until the lobe eventually retreated from the Strait of Juan de Fuca, and the Puget Sound connected once again with the Pacific Ocean (Booth, 1987; Troost and Booth, 2008). With the weight of the ice sheet removed, the crust rebounded and sea level also changed (Booth, 1987). These relatively rapid changes likely created weaknesses within the sediments of Steamboat Island Peninsula.

Furthermore, earthquakes caused by subduction and thrust movement along the 285°-striking Olympia Structure are hypothesized to have cut faults through Pleistocene and Holocene sediments of the northern Steamboat Island Peninsula (Clement et al., 2010) (Figure 3). The 2001 Nisqually Earthquake reactivated landslides and created liquefaction features on the peninsula (Malone et al., 2001; Lasmanis, 2001). Finally, anthropogenic climate change is causing sea level rise and storm intensity (Mauger et al., 2015), both of which trigger landslide movement.

Previous Inventories and Landslide Protocols

Landslide Inventories

Landslide inventories are created to: 1.) document slope failures (Shipman, 2001; Guzzetti, 2005; Burns and Madin, 2009; Guzzetti et al., 2012), 2.) show hazards and calculate risk (Shipman, 2001; Guzzetti, 2005; Burns and Madin, 2009; Guzzetti et al., 2012), 3.) record impacts of storm events or earthquakes (Gerstel et al., 1997; Shannon and Wilson, 2000; Malone et al., 2001; Shipman, 2001; Guzzetti, 2005; Sarikhan et al., 2008; Guzzetti et al., 2012), 4.) provide a record of human and financial losses (Guzzetti, 2005); and 5.) calibrate probability and slope stability models (Shipman, 2001; Baum et al., 2005; Guzzetti, 2005; Booth et al., 2009; Guzzetti et al., 2012). Landslide inventories are maintained at different levels (local, state, national) and in different formats. Efforts to create a worldwide database began in the 1990s with the United Nations Education, Scientific, and Cultural Organization (UNESCO) Working Party on World Landslide Inventory (Guzzetti, 2005). Today, National Aeronautics and Space Administration's (NASA) Goddard Space Flight Center (GSFC) keeps a database of rain-triggered landslides to understand human and financial losses and climate change impacts (Kirschbaum et al., 2009). While these larger databases are useful for research, national and statewide inventories are more practical for funding, mapping, and understanding local hazards and risks, and they can eventually feed into larger databases. The United States Geological Survey (USGS) has an inventory pilot project (http://landslides.usgs.gov/research/inventory/), which involves twelve states, including Washington and Oregon. However, none of these states have completely finished mapping landslides at a 1:24,000 or

larger scale for the entire state; only California, Colorado, and Oregon have an easily accessible GIS interface with detailed information on the mapped landslides.

DOGAMI Protocol

The DOGAMI protocol developed out of a larger USGS project. Many of the same winter storms (1996-97, 1998-99, and 2006-07) that caused numerous landslides in Washington hit Oregon equally as hard (Gerstel et al., 1997; Shipman, 2001; Burns, 2007; Sarikhan, et al., 2008). With limited money and resources, DOGAMI investigated the usefulness of remote-sensing datasets to communicate landslide hazards to the public and cover large portions of Oregon with greater spatial resolution (Burns, 2007). Geologists digitized landslides using one of the following data sets: 1.) a Digital Elevation Model (DEM) resolution from the Shuttle Radar Topography Mission at 30m, 2.) a DEM from USGS topographic quadrangles at 10m, 3.) photogrammatic and ground based elevation contours at 1.5m (5ft) interval resolution, 4.) stereo-pair aerial photographs, and 5.) a lidar DEM at 1m resolution. DOGAMI found that lidar mapping at 1m resolution took longer but was necessary for accurately locating and documenting landslides of multiple sizes. However, they also noted that lidar could not be used in isolation, and that previous landslide studies, orthophotos, aerial photos, and mapper experience mattered in making a complete inventory.

Landslide Inventories within the Puget Sound

While not a landslide inventory, Hugh Shipman (2001) compiled photos and brief descriptions of the most destructive coastal landslides on Puget Sound during two years of intense storms:1996/97 and 1998/99. This survey points out that periodic, intense rainfall during 1996/97 resulted in several shallow landslides, while steady, less intense rainfall in 1998/99 reached a three-month record and reactivated deep-seated landslides. Both the Carlyon Beach/Hunter Point Road landslide and the Sunrise Beach Road landslide moved in February of 1999, damaging over sixty homes (Figure 4).

The storms of 1996/97 also prompted Seattle Public Utilities to contract Shannon and Wilson to make a comprehensive inventory of the landslides in Seattle, WA (Shannon and Wilson, 2000). Once complete, their inventory identified 1,326 landslides (Shannon and Wilson, 2000). Shannon and Wilson (2000) used GIS to map the landslides on a DEM derived from topographic maps of the area, recording the date of movement, type of movement, geologic conditions, and possible contributing factors. They field-checked the identified landslides to reduce the error in location, and they represented all landslides as dots (placed at the top and center of the scarp) on large-scale maps (from 1 in = 1500 ft. to 1 in = 2640 ft.). For reasons they do not specify, they departed from the traditional Cruden and Varnes (1996) classification system used by most landslide protocols, including DOGAMI's, and they defined the landslides as either: 1.) high bluff peeloff; 2.) groundwater blowout; 3.) deep-seated landslides (rotational

and translational); and 4.) shallow colluvial (skin slide) (Shannon and Wilson, 2000). Their inventory provided the foundation for several future landslide studies on local susceptibility (Schulz, 2007) and modeling hazards (Baum et al., 2005).

Prior to DGER (2009) mapping of Thurston County, the USGS team of McKenna, Lidke, and Coe (2008) mapped the entirety of Kitsap County, using only lidar data and four days in the field. They acquired their lidar imagery from the Puget Sound Lidar Consortium (PSLC), which flew the project in 2000 during the leaf-off season (http://pugetsoundlidar.ess.washington.edu/lidardata/restricted/projects/2000-05lowerpugetsound.html). The DEM grid-cell size is 1.8 m (6 ft.), which is the same resolution the DGER (2009) team used. While McKenna et al. (2008) did not use aerial photos or any other non-GIS data sets, they did produce the same types of derivatives from the lidar that Burns and Madin (2009) call for in their protocol—topographic contours, slope, and hill-shaded relief with varying sun angles. McKenna et al. (2008) also digitized at scales from 1:5,000 to 1:2,000, and then they compared their results to previous landslide maps of the county. They found that lidar imagery is best for locating moderate (250-10,000 m^2) to large (>10,000 m^2) landslides, and that the majority of the moderate landslides are located at the north end of Kitsap County. Importantly, they noted that aerial imagery and field work were required in addition to lidar to map the smallest landslide (252 m^2); however, lidar imagery still allowed them to map twice the number of landslides identified by previous geologists.

Other lidar mapping efforts in the Pacific Northwest reported finding two to four times more landslides than previous efforts that relied solely on aerial photographs and fieldwork (Haugerud et al., 2003; Schulz, 2007). Therefore, comprehensive inventories should be compiled using lidar, previous work, aerial photos, shoreline photos, and field work. The DGER (2009) inventory is one such inventory for Thurston County's marine shore.

DGER (2009) Thurston County, Washington landslide inventory

During 2006 to 2007, principal investigator Michael Polenz led a team that mapped this area in detail (DGER, 2009). The team did most of its identification and mapping of landslides working from a boat. Additionally, the team used reconnaissance reports, geologic maps, aerial photos (from 1936 to 1977), 2003 orthophotos, 2000/2001 oblique shoreline aerial photos from the Washington State Department of Ecology, 2005 10m DEM bathymetry from the University of Washington School of Oceanography, and 2002 1.8m (6ft) resolution lidar from the PSLC. In ArcGIS 9.x, they derived slope, contour, hillshade, and SMORPH (ESRI slope stability software available at http://arcscripts.esri.com/details.asp?dbid=15095) layers. Although, they digitized at other scales, the DGER team notes that the final map product is precise at only a 1:12,000 reference scale. Furthermore,

they warn that some shorelines received more attention than others because of factors such as land access and available data quality. The DGER team created their own protocol for this project, and they kept a thorough log on each of the landslides they mapped as a supplement to the 38 fields of the attribute table stored in a GIS database. In addition to the standard information collected about landslides (the landslide type, date(s) of movement, area, certainty, etc.), they also recorded the existence of sag ponds and springs, types of vegetation, presence of large woody debris along the shore, names of previous researchers, and the specific photo numbers used as part of the identification process. The thoroughness of their project is the reason I used it as the dataset to compare my work against.

Technical Reports for Steamboat Island Peninsula landslides

After the rainstorms of 1998/1999, two large landslides reactivated on Steamboat Island Peninsula (Figure 4). Thurston County hired GeoEngineers (1999) and Shannon and Wilson (1999) to perform Phase I and II investigations on these movements. I used their borelogs, geologic descriptions, maps, and cross sections for my inventory.

Carlyon Beach/Hunter Point Road Landslide by GeoEngineers (Figures 4 and 5)

February 6, 1999, residents within the Carlyon Beach Estates noticed cracks and settlements in streets and driveways, and eventually 41 homes experienced enough shifting and distress that they were deemed unsafe for occupancy. As GeoEngineers looked back through previous geotechnical work within the neighborhood, they realized movement within the landslide began as early as 1996. In order to characterize the movement, GeoEngineers drilled 22 geotechnical soil borings, and installed twelve inclinometers and ten water piezometers (Figure 5). Their work revealed that a dense, silty fine to medium sand (interpreted as advance outwash, Qga) is exposed in the head scarp and proceeded to depths of 15m (50ft) in the soil borings. Conformably below the sand, they discovered stiff to hard, silt, silty clay and clay, which varies in thickness from 43m (140ft) in the western portion of the landslide to 61m (200ft) in the eastern portion. At the toe of the landslide, they found this unit with evidence of shearing from past ground movement. Below the silt and clay unit, they encountered sand and gravel, which dips toward the northeast. They explain this coarser sediment as an older glacial or interglacial period (probably Qps).

Almost two months after movement initiated, the landslide continued moving, crimping and shearing seven of the inclinometers. These movements occurred at different depths, ranging from 9.8m (32ft) to 32m (105ft). Using 50 control points to measure movement within the slide, GeoEngineers found the largest horizontal movement to be near the waterfront of the central portion of the landslide, with a maximum of 0.427 ± 0.003m (1.40 ± 0.01ft). The largest vertical displacement was 0.13 ± 0.003m (0.43 ± 0.01ft) near the head scarp.

Due to this continued movement, GeoEngineers provided short-term and long-term recommendations. The short-term recommendations involved Thurston County evacuating homes, shifting Hunter Point Road to the south, removing at-risk trees, and installing emergency shutoff valves to water lines. Their long-term recommendations (several found in Phase II investigations) were analyzed and had the potential to increase the factor of safety (FOS) from 1.1 to 1.4 depending on which course of action the community selected. As these options ranged in price from $140,000/home to $723,000/home, the community chose not to do any remediation (Shipman, 2001).

Sunrise Beach Road Landslide by Shannon and Wilson (Figures 4, 6-8)

The same above-average rainfall that reactivated the Carlyon Beach/Hunter Point Road landslide also reactivated a landslide along the southeast shoreline of Eld Inlet known as Sunrise Beach Road landslide (Shannon and Wilson, 1999) (Figures 4 and 6). Initially, extension cracks opened up along Sunrise Road, then the landslide began to damage homes, driveways, and sewage pipes. By March 31, 1999, Thurston County Department of Roads and Transportation Services authorized Shannon and Wilson to continue their investigation from Phase I and proceed to Phase II, which involved evaluating borings, installing inclinometers, conducting groundwater studies, and providing a recommendation on how to mitigate the landslide.

In order to define the geology, planes of weakness, and water flow, Shannon and Wilson drilled five borings (Figure 6). They found that surficial, glacial sediments differ on either side of Sunrise Road, whereas a thick layer of hard silt and clay, interpreted as glaciolacustrine deposits (they note as Qvgl, but it is Qga on 7.5-minute Tumwater Quadrangle) is common to both sides. The cross section in Figure 7 shows the glacial sediments involved in the landslide.

Shannon and Wilson (1999) determined that three aquifers exist in the vicinity of the landslide. The dense sand of the advance outwash (Qva) and the looser sand of the recessional outwash (Qvro) are unconfined aquifers, but the pre-Vashon sediments (Qpnl, Qpnf, and Qpgo) are a confined aquifer. Shannon and Wilson's (1999) observed interactions between the unconfined aquifer flows and the landslide features and materials suggested that the failure occurred due to pore water pressure building among the advance outwash, the recessional outwash, and the glaciolacustrine silt and clay. Drillers lost 150 gallons of drilling mud at a depth of 15m (50ft) in borehole 3 (B-3), and Shannon and Wilson interpreted the landslide's rotational plane from the head scarp to this depth (Figures 7 and 8).

To remediate the landslide and increase the FOS, Shannon and Wilson (1999) recommended lowering the groundwater table. They proposed a 6m (20ft) deep trench to extend along Sunrise Road and capture water from the advance outwash flowing into the recessional outwash. Furthermore, they suggested

installing horizontal drains into the steep slope west of the road and into the seawall. The cost of their recommendations came out to just over $1.2 million dollars. Responsible for fixing the road, Thurston County joined the residents living along this section of the road in sharing the price of the project. Three residences also invested in soldier pile walls to protect their homes (Shipman, 2001; personal communication with Mark P. Biever of Thurston County Water and Waste Management, 2016).

Nisqually Earthquake, 2006/07 Storm, and the Sunrise Beach and Hunter Point Road Long Term Monitoring Plan

On February 28, 2001 at 1054 PST a magnitude 6.8 earthquake shook the Puget Sound region and created several landslides within the area (Malone et al., 2001; Lasmanis, 2001). A few significant landslides occurred in Thurston County; one happened below the state capitol in Olympia, and the other just southeast of my mapping area along US101. Serendipitously, the day prior to the earthquake, a geologist read the inclinometers left at Sunrise Beach Road landslide as part of a long-term monitoring program, and he returned the day after (personal communication from Mark P. Biever to Thurston County's Department of Roads and Transportation Services, 2005). Between February 28, 2001 and June 18, 2001, borings 1, 2, and 3 (Figure 6) all registered small shifts – with a maximum of 0.33cm (0.13in) – perpendicular to Sunrise Road (Table 2). The accuracy of the inclinometers is to the one-thousandth of an inch, so this is actual movement (personal communication from Mark P. Biever to Thurston County Roads and Transportation, 2000).

While the Nisqually Earthquake did not cause any shifts near the inclinometers left at Hunter Point Road (personal communication from Mark P. Biever to Thurston County's Department of Roads and Transportation Services, 2005), it did reactivate the Carlyon Beach/Hunter Point Road landslide (Lasmanis, 2001). The same slide also moved again with the rainstorms of 2006/2007 (personal communication Mark P. Biever to representatives of Thurston County, 2007). This time, members of the Carlyon Beach Homeowners Association noticed cracks opening in the streets, but they did not report any further damage. That same winter, the Sunrise Beach Road landslide remained inactive.

Data Sources

In order to investigate my hypothesis, that I can use the office-centered protocol developed by Burns and Madin (2009) to identify landslides along the coastline of Steamboat Island Peninsula and that the area mapped will reasonably agree with the field-based map created by the DGER (2009), I followed the steps of the DOGAMI protocol. At a minimum, the DOGAMI protocol requires the following:

i. Acquire DEM derived from lidar data,
ii. Create a slope map from the lidar data,

iii. Gather orthorectified aerial photos of similar age to the lidar data,
iv. Find previous landslide inventories or other data on landslides within the mapping area, and
v. Obtain geologic maps.

Table 3 summarizes the sources of data I used in order to map the shoreline landslides around Steamboat Island Peninsula.

Lidar Data

I selected lidar data flown in June and July of 2011, seven years after the lidar data used by the DGER team for their inventory, because it is at a higher resolution (1m vs. 2m) and meets newer standards from Federal Emergency Management Agency's (FEMA). In January of 2009, the Chehalis River flooded and shut down Interstate 5. As the earlier lidar flown by the PSLC did not meet the standards for mapping floodplain hazards, Thurston County partnered with FEMA to acquire more accurate lidar and contracted with Fugro Earth Data, Inc. to do the work (personal communication with Owen F. Reynolds, GIS Analyst at Thurston Geodata Center, August 2015).

Using the Leica ALS60 MPiA LiDAR system (107,500 to 126,200 pulses per second), Fugro Earth Data, Inc. flew night passes during the leaf-on season to collect the lidar data (Thurston Geodata Center, 2012). Fugro monitored the positional dilution of precision (PDOP) with a global positioning satellite (GPS) base running at the Olympia Airport (Thurston Geodata Center, 2012). After the flights, Fugro combined the GPS data from airport with the aircraft's GPS and inertial measurement unit (IMU) data to create accurate positions and altitude angles. With this position data, Fugro processed the raw lidar data with TerraScan software and its own proprietary software. Therefore, the lidar data (in flat, non-vegetated areas) has a horizontal position accuracy of 18.2cm (7.17in), and a vertical position accuracy of 15-18cm (6-7in) (Thurston Geodata Center, 2012; personal conversation with Owen F. Reynolds, May 2016).

Orthorectified Aerial Photos and Aerial Photo Sets

The Washington State Geospatial Data Archive (WAGDA) provides downloadable National Agriculture Imagery Program (NAIP) aerial photography processed to use with GIS. I obtained 4-band, 1-meter resolution NAIP imagery from 2009, 2011 (same year as lidar data), and 2013. For historical aerial photos, the Washington DGER provided me with five series flown in 1965 (1:12,000 black-and-white), 1971 (1:66,000 black-and-white), 1972 (1:66,000 black-and-white), 1976 (1:24,000 color), and 2003 (1:12,000 color). I viewed the 1965 and 2003 photos stereoscopically. For oblique views of the shoreline that show the face of the bluffs and provide evidence of smaller movements, I used the Washington State Department of Ecology's Coastal Atlas Map (https://fortress.wa.gov/ecy/coastalatlas/tools/Map.aspx).

With a tool they provide on their website, I compared photos from 1977, 1992-1997, 2000, and 2006. From this site, I downloaded photos that showed evidence of shoreline change.

Previous Landslide Inventories

As mentioned in the section on previous work, I used GeoEngineers' (1999) technical report on the Carlyon Beach/Hunter Point Road landslide and Shannon and Wilson's (1999) technical report on the Sunrise Beach Road landslide (1999) to map scarps and deposits, and complete fields within my attribute table. I updated the last movement of landslides from Malone et al.'s (2001) and Lasmanis' (2001) article on the Nisqually earthquake landslides. I also met with Mark P. Biever in Olympia, who provided information on inclinometer data and the details of the remediation at the Sunrise Beach landslide and took me to see both landslides (personal communication, March 2016). Although I obtained the DGER (2009) landslide inventory at the onset of the project, I did not open or engage with it until after I independently mapped all of the landslides and populated the attribute table according to the DOGAMI protocol.

Geology Maps and Well Log Data

For the geology of the area, I referred to four 7.5-minute quadrangle maps: 1.) Summit Lake (Logan and Walsh, 2004), 2.) Shelton (Schasse et al., 2003), 3.) Squaxin Island (Logan et al., 2003), and 4.) Tumwater (Walsh et al., 2003). Additionally, I downloaded the GIS database of the DGER's 1:24,000 scale geologic map (2014). For well log data and locations, I used the Department of Ecology's website portal, "Well Logs" (https://fortress.wa.gov/ecy/waterresources/map/WCLSWebMap/WellConstructionMapSearch.aspx).

Methods

My hypothesis is that following the DOGAMI protocol will generate an accurate, reproducible landslide map and inventory of the shoreline landslides along Steamboat Island Peninsula. In order to test my hypothesis, I followed the DOGAMI protocol (Burns and Madin, 2009) and compared my results to the field-based map and landslide inventory created by the DGER (2009). This test is successful if my landslide area matches with the landslide area mapped by the DGER (2009).

Therefore, using ESRI's ArcGIS 10.2.2, I mosaicked the DEM raster files that cover Steamboat Island Peninsula. From the DEM, I created two hillshade maps, both with the default sun altitude of 45°, but one with a sun azimuth of 315°and the other of 45°. I made a slope map, and reclassified the data, as specified by the DOGAMI protocol, to emphasize slopes greater than 45°. From the DEM, I also created a 6m (20ft) contour layer, and a slope aspect layer; the DOGAMI protocol doesn't specifically call for an

aspect layer, but it becomes useful when specifying the direction the landslide moved. Finally, I added the NAIP orthorectified layers, and the DGER (2014) surface geology layer.

Next, I created the landslide inventory geodatabase and formatted the spatial and tabular data. For the spatial data, I established the four feature classes: 1.) deposits (polygon), 2.) scarp flanks (polygon), 3.) scarps (lines), and 4.) photos (points). I set up the detailed attribute table in the deposits feature. The 24 unique fields are outlined in Table 4 and described in further detail in Appendix A of the DOGAMI protocol (Burns and Madin, 2009).

The DOGAMI protocol relies on several definitions to fill the fields of the attribute table. The fields focused on the type of movement and classification of movement come from modifications of Cruden and Varnes (1996). Thanks to the early work of Varnes (1978), and the updates from his colleague Cruden (1996), most of the world is using the same set of definitions (Guzzetti et al., 2012; Hungr et al., 2014). As I mapped, I adhered to and recalibrated with these definitions, which are:

- ***Landslide*** refers to "the movement of a mass of rock, debris or earth down a slope" (Cruden and Varnes, 1996).
- ***Material*** is rock or soil (Varnes, 1978; Cruden and Varnes, 1996).
- ***Rock*** *(bedrock)* is "a hard or firm mass that was intact and in its natural place before the initiation of movement" (Cruden and Varnes, 1996).
- ***Soil*** is "an aggregate of solid particles, generally of minerals and rocks, that either was transported or was formed by the weathering of rock in place" (Cruden and Varnes, 1996). ***Soil*** is further broken down into earth and debris:
    - ***Earth*** is "material in which 80 percent or more of the particles are smaller than 2mm (0.08in), the upper limit of sand-size particles;"
    - ***Debris*** is "20 to 80 percent of the particles are larger than 2mm (0.08in)" (Cruden and Varnes, 1996).

The distinction between *earth* and *debris* is challenging in a glacial environment with only remote sensing. Therefore, where till or gravels are mapped, mentioned in a profile or bore log, or part of a nearby well log, I considered the material *debris*. However, if sands from glacial outwash or recession, and/or silts and clays from glaciolacustrine deposits are involved, I considered the material *earth*.

When it comes to the types of landslide movements, the only other term that needs to be defined is ***complex***, which was dropped from the Cruden and Varnes (1996) type of movement, but retained as a descriptor of activity. However, Burns and Madin (2009) defined it as "combinations of two or more types." I used this definition, and then attempted to clarify which two types appeared to be involved. For

example, GeoEngineers (1999) considered the recent motion within the Carlyon Beach/Hunter Point Road Landslide to be translational; however, based on multiple, back-rotated blocks and sag ponds, I interpret it as a rotational landslide. Therefore, I mapped it as a complex, translational>rotational (translational movement greater than rotational movement). As Varnes (1978) pointed out, "rigid classification is neither practical nor desirable." Within an inventory protocol, the term "complex" allows for this flexibility.

Another assumption within the DOGAMI protocol is that weathering over a small region (such as a county) is roughly equal. Therefore, the sharpness or roundness of landslide features tells us about the landslide's age (e.g., Burns and Madin, 2009; LaHusen et al., 2015). Within my area, I attempted to pin-point the movement as either ***modern***—I have a report documenting actual movement or I can show two pictures with different dates and a change in the slope—or ***historical***—I cannot document the movement and it's large enough that it took significant time to form. This differs slightly from how Burns and Madin (2009) define estimated age in their protocol. They use Oregon statehood as the dividing line between active and/or historic (movement <150 years) and prehistoric or ancient (movement >150 years).

Finally, I worked clockwise around Steamboat Island Peninsula, digitizing the landslides. In supplement to the protocol, I digitized the landslides in multiple iterations, collected Department of Ecology photos and well logs, and highlighted scarps and other features in oblique aerial photos (Figure 9).

Assumptions

One of the major assumptions about mapping landslides from remote data is that the landslide event leaves a morphologic signature that a trained geologist or automated mapping program can distinguish (Guzzetti, 2005; Booth et al., 2009; Guzzetti et al., 2012). These morphologic signatures include steep, concave scarps, sag ponds, back-rotated blocks or hummocks, runout fans, and talus slopes. Furthermore, specific morphologic signatures are used to determine the overall type of movement (Varnes, 1978; Cruden and Varnes, 1996; Guzzetti et al., 2012). An example is large, back-rotated blocks below a steep head scarp, which many geologists would identify as a deep-seated, rotational landslide.

Another assumption I made is about the adherence to the DOGAMI protocol. I assumed that geologists at DOGAMI use the protocol scoring system rigidly for determining confidence in landslide identification. Therefore, I created a spreadsheet to tally and record my confidence levels (Appendix A). In further discussing how to assign the confidence level, Bill Burns explained that this portion of the protocol is not to be rigidly followed, but rather to calibrate oneself with known landslides (personal conversation, April 2016). For instance, the Carlyon Beach/Hunter Point Road landslide is known to move, so features that

look like it could be ranked as high. By the time I had this conversation, I was too far into my mapping to make changes; therefore, I left the tallies and confidence levels.

Results and Discussion

Results using the DOGAMI protocol along Steamboat Island Peninsula

Using the DOGAMI protocol, I mapped approximately 40-50 km (25-30 miles) of shoreline from my desktop computer running ArcGIS 10.2.2. I mapped 36 landslide deposits and 48 recent events within these deposits (photo points), covering a total disrupted area (both the scarps and deposits) of 879,530 m^2 (9,467,160 ft^2) (Table 5; Figure 4). The largest landslide is 'Squaxin 6', better known as the Carlyon Beach/Hunter Point Road landslide, with a total deposit area of 169,870 m^2 (1,828, 450 ft^2), and a total disrupted area of 183,740 m^2 (1,977,780 ft^2). The smallest is 'Tumwater 2'. As a flow without a discernable scarp, it has both a total deposit area and total disrupted area of 140 m^2 (1,470 ft^2). Two other possible movements that I could not satisfactorily verify are not counted in this tally, but show up on the map as photo points.

The first tabular data collected is the type of movement and the classification of material and movement types (Burns and Madin, 2009) (Table 6). I found ten complexes, twenty-three slides, two topples, and one flow (Tables 6 and 7). Within the complexes, I identified more debris slides with a greater component of rotation than translation. Slides have the highest overall total, with translational debris and earth slides the most common in this category. Topples and flows are likely lumped into larger movements or missed altogether because their signature is challenging to pick out on the lidar. This is partially due to the size of these movements which need to be larger than a few meters to be revealed by 1m lidar, and partially due to the algorithm which removes the vegetation (Haugerud et al., 2003), but creates facets along the steep shoreline.

The DOGAMI protocol uses a scoring system to determine confidence in identifying a landslide. It ranks confidence for each of the following features—head scarp, flanks, and toe—on a 0-10 basis, for a maximum of 30 points. Internal scarps, sag ponds, and/or compression ridges are also ranked 0-10, but only once. Therefore, the total maximum score is 40. High confidence is defined as >30 points and/or a documented account of movement; medium confidence is defined as 11-29 points; and low confidence is $\leq$ 10 points. I found that all of the landslides I identified fell into the medium category. The only exceptions are the Carlyon Beach/ Hunter Point Road and Sunrise Beach Road landslides. Without bathymetry data and due to continuous wave erosion and drift cell motion, I consistently ranked the confidence for the landslides' toes as one or two, which brought the overall score down to medium confidence (Appendix A).

As I mentioned in the Methods section, I deviated from the protocol when estimating the age or time the landslide moved. I used the terms 'modern' and 'historic', and both terms if I found photographic evidence of smaller movement within the larger landslide. I found only two landslides to be historic, thirteen both historic and modern, and eleven modern (Table 8). Furthermore, I documented every instance where I found movement, which shows that the Carlyon Beach/ Hunter Point Road Landslide is the most active complex. It also shows that, with the exception of very slight movement recorded only by inclinometers during the 2001 Nisqually Earthquake, the remediation of the Sunrise Beach Landslide is working to stabilize that slope (Table 2).

In addition to determining when the landslides moved, it is important to know what material is moving. For each landslide, I used the 7.5-minute quadrangle maps and cross sections, and I also found the nearest well logs from the Washington Department of Ecology (Appendix A provides well log names; Figure 4 shows locations). From these twenty-one well logs, the maps, and my estimation to the failure plane, I found that glacial till (Qvt/Qgt), advance outwash (Qva/Qgas/Qga), glacial lacustrine fines (Qvgl/Qpf), pre-Vashon sands (Qps), and pre-Vashon gravels are likely within the stratigraphy of the failure (Figure 10). The Shannon and Wilson (1999) and GeoEngineers (1999) technical reports provided me with the most accurate interpretations for the geology of the failures and the depth to the failure plains.

To find the average slope of the hillside prior to the landslide, I created 85 profile lines, making one near each flank scarp or deposit edge. The odd number of profile lines is due to the fact that some landslides do not have an adjacent flank next to their scarp; in fact, another landslide often cuts across the same area or erosion makes the flanking slope unrecognizable. The accuracy of the angle is within a degree or two because the measurement of the angle uses the arctangent of the difference in height along the vertical distance. With this rough estimate, I found 'Squaxin 6' (Carlyon Beach/Hunter Point Road) and 'Squaxin 8' to be the shallowest failures, with an average slope before failure of 10°; 'Summit Lake 3c' is the steepest failure, with an average slope of 36° (Table 9). The shallowest slopes are classified as deep landslides, and the transition to shallower landslides is around a slope angle of 20°. Depth is set by the protocol at 4.5m (15ft); Burns and Madin (2009) use this number based on previous studies of colluvium to bedrock depth, and due to the fact that most construction sites go to this depth for excavations. Making these profile lines can be tedious, and with zonal statistics, a GIS system can be programmed to calculate the internal slope of the landslide. The difference between the profile calculations and the internal slope is minimal.

To calculate a simplistic volume of the landslides (based on a translational landslide's geometry), it is also necessary to know the height of the scarp (from the top of the undisturbed slope to the top of the disturbed material) in order to find the slope normal thickness of the slide. I could only identify a clear

scarp on fifteen landslides; therefore, I made 37 small profile graphs so that I could calculate the average head scarp height. While not discernable on the lidar, Shannon and Wilson (1999) measured the Sunset Beach Road landslide to have a 1m (3ft) scarp. The highest head scarp I found is 13m (43ft) at 'Squaxin 7'; however, most of the landslides with an identified scarp have an average height of 8m (25ft). This simplistic estimate of volume puts the Carlyon Beach/ Hunter Point Road landslide as the largest, and 'Tumwater 5' as second largest (which contains Sunrise Beach Road landslide).

While the protocol also calls for measuring the distances between internal scarps and secondary scarps, I did not make these measurements. I did digitize a few internal scarps, but due to the algorithm that removes the vegetation (Haugerud et al., 2003), these internal scarps are challenging to trace for any distance (Figure 11).

Finally, the protocol uses a sixteen spoke compass rose to help determine the direction of motion. I used an imaginary line drawn through the center of the landslide and perpendicular to the head scarp and compared this azimuth to the compass in the protocol. Additionally, I used the ArcGIS aspect tool on the lidar- derived DEM, and compared this overall aspect of the entire landslide to my single azimuth selection. This is another step of the DOGAMI protocol that a geologist can automate with GIS, saving time. The majority of landslides failed into the west-northwest quadrant (18 landslides), and east-southeast quadrant (14 landslides) (Table 10). These directions fit with the orientation of the peninsula, and probably a larger structural weakness within the area (Logan and Walsh, 2004).

Results and Discussion comparing this study to the DGER (2009) inventory

The objective of my research is to use the DOGAMI protocol to map landslides along the shoreline of Steamboat Island Peninsula, compare and contrast my results to the DGER (2009) dataset for this same shoreline, and recommend improvement for future landslide inventory creation. I found 36 landslide deposits and 48 recent movements within these slides (photo points). Along this same 40-50 km (25-30 miles) stretch of shoreline, the DGER recorded 264 landslides; however, several of these slides overlap or are contained within a larger complex. Accounting for this overlap, their total number of landslides reduces to 159.

These 159 complexes cover an area of 3,256,570 m^2 (35,053,400 ft^2). The 36 landslides and complexes I mapped cover a total area of 879,530 m^2 (9,467,160 ft^2), leaving a difference of 2,377,040 m^2 (25,586,240 ft^2). For three of the DGER landslides, I lacked either lidar coverage (DGER slide ID 3) or bathymetry data (DGER slides 40 and 521 are entirely covered with water). These three slides account for another 370,100 m^2 (3,983,720 ft^2), decreasing the difference between my mapped landslide area and the DGER's mapped area. However, area alone does not tell the entire story.

To further understand the differences, I created a field within the DGER attribute table (titled "DML Evaluation") and evaluated each of the 264 entries. For 122 of the DGER landslides, my data overlapped with the DGER, but I either lumped slides together or I split them apart. For example, within my 'Squaxin Island 2' landslide, the DGER mapped 6 individual slides (Figure 12a and 12b). However, the DGER also mapped a much larger swath, which contains my 'Squaxin Island 2' and other slides I did not identify (Figure 12c). For 107 landslides I classified with a version of "Understand; steep slope," which means I did not map these slides, but I recognized these slopes as steep and resulting from erosion and mass wasting (Figure 13a). Without a photo or second piece of evidence to show recent slope movement, I left these areas unmapped, or in a few instances just a photo point.

I did not identify the remaining 35 landslides for a variety of reasons (Table 11). As mentioned above, two slides are underwater and one is outside the lidar coverage. Seven slides I did not recognize because humans have altered and modified the landscape, building roads and homes that grade over scarps or fill hummocky topography ("Too modified") (Figure 13b). Nine I interpreted as fluvial processes dominating, and I marked as "Fluvial," with a further explanation (Figure 13c). Four of the landslides the DGER identified, I disagree with ("Disagree; …") because the area they digitized is either flat or has a ridge through the middle (Figure 14). The final twelve landslides did not fit neatly into one of the above categories.

Once I went through the 264 individual slides, I looked for trends between the certainty of the DGER slides and the landslides I mapped (Table 12). The DGER mapped 123 slides with 'definite' certainty, covering a total area of 658,160 m^2 (12,740,500 ft^2). While I mapped only 56% of the same area within my inventory, four of their landslide complexes extended into the water, with the toes covering almost as much area as that mapped on land (Table 13). Of the landslides with the largest area that they classified as 'probable', one is outside of my lidar coverage and two are in the highly modified valley to the west of the Carlyon Beach/Hunter Point Road landslide. Otherwise, the 30% overlap is due to several small slides falling along the steep slopes, which I recognized but did not map as a deposit.

A significant area, 2,093,860 m^2 (22,538,150 ft^2), of the slides identified by DGER is defined as 'questionable.' I agree that these landslides are questionable, and I had only 5% overlap. Given that this much area is questionable and including the three slides outside of my data set 370,100 m^2 (3,983,720 ft^2) puts my total area of 879,530 m^2 (9,467,160 ft^2) much closer to the area mapped by the DGER. In fact, subtracting the questionable area (which includes the area outside my data set) and the area within the toes (bathymetry required) from their total area, the DGER mapped 872,950 m^2 (9,396,320 ft^2) with certainty (Table 13). This makes the difference, 6,580 m^2 (70,840 ft^2), almost equal.

Our studies have the highest agreement in the category of 'Prior account, but unverified by the compiler' (DGER, 2009). First of all, this category and the next category, 'Prior account, verified (by the compiler)' cover the least amount of area. Four smaller slides within the Carlyon Beach/Hunter Point Road landslide fell into an area already known to be moving. Two others fell into 'Squaxin Island 11,' which I knew about from 7.5-minute quadrangle for Squaxin Island (Logan et al., 2003). Finally, I have 40% overlap with the last category, 'Prior account; verified,' because several smaller slides are within larger slides I mapped from the same 7.5-minute quadrangle. The exception is a medium landslide that is not on a quadrangle, and along a modified beach front. While I did not map as many individual landslides as the DGER, I have higher than 50% overlap for the 'Definite,' 'Prior account, but unverified by the compiler,' and 'Prior account-verified' landslides; I did not have significant overlap with the 'questionable' landslides.

Most inventories not only want to show where landslides are located, but also what type they are because this observation provides an indication of the hazard's risk (Shipman, 2001; Baum et al., 2005; Schulz, 2007; McKenna et al., 2008; Guzzetti et al, 2012). The DOGAMI protocol classifies landslide movement type and material based on the previous work by Cruden and Varnes (1996). In making their inventory, the DGER used terms from Cruden and Varnes (1996), but also added terms from the Shannon and Wilson (2000) inventory of Seattle landslides. Therefore, the DGER came up with twelve types of movement, shown in Table 14. As this is not a one-to-one comparison, I found it challenging to evaluate how much my work agreed or disagreed with the DGER inventory. Further complicating this differentiation is that I merged several failures together (i.e. the long, western coastline of the peninsula that I identified as 'Squaxin Island 4pt2'). What I ultimately show in Table 14 is that roughly 50% of my landslide identifications match with the DGER identifications. In some areas this correspondence is higher because they went with no description or an open description (i.e. other or blank), but I did not identify any earth flows, and they found three. Also, the descriptor "deep" correlated at a higher frequency than the descriptor "shallow." Working remotely, as in my case, 4.5 m (15ft) is a challenging determination unless the slope has greater than a 4.5 m (15ft) drop within 5.5 m (18ft), or if something within the picture provides a known scale. Therefore, it is easier to determine deep landslides versus shallow.

While the DGER team created their inventory in the field, they did so from a boat, and they field-checked only 22 of the slides along the Steamboat Island Peninsula shoreline. While they did not limit their interpretation of the geology to only these landslides, they only expanded to 112, using outcrops, technical reports, and 7.5-minute quadrangles. As I did not conduct field work, I completed my interpretation from the same 7.5-minute quadrangles, technical reports, and an additional 21 well logs.

Well logs are not as accurate as borehole data because the logger is not always a trained geologist. Also, glacial sediments are not deposited in continuous, uniform layers; therefore, a well log is a very rough estimate of the geology of these landslides. In cases where the material of a landslide does not need to be known in great detail, geologic maps and well logs can suffice, but landslides that have the potential to impact humans should be field checked.

This challenge of classifying landslide types in not limited to this study. In fact, recent work by Hungr et al. (2014) attempts to update the Varnes classification by using geotechnical and geological terms. Their update is backward-compatible, and it drops the term "earth" and adds descriptors taken from the Unified Soil Classes (Hungr et al., 2014). The final result is six general types of movement (falls, topples, slides, spreads, flows, and slope deformations) with a total of 32 specific types (Table 15). While the term "complex" is dropped from the 32 specific types of movement, Hungr et al. (2014) leave room for users to combine terms as needed. Furthermore, they add a classification that applies to actively eroding slopes along shorelines and riverbanks (Hungr et al., 2014); this classification solves my dilemma with lumping landslides such as 'Squaxin Island 4pt2.' These types are much more in line with the various movements found on Squaxin Island Peninsula.

Conclusions and Recommendations

This study used the DOGAMI protocol to create a landslide inventory for Steamboat Island Peninsula, and compares the results to the DGER (2009) inventory. As I hypothesized, this office-centered protocol can effectively identify landslides on high-resolution lidar, as shown by my mapped area nearly equaling the DGER's (2009) mapped area (Table 13). It is especially accurate when paired with the other data sources Burns and Madin (2009) suggest in the protocol, such as aerial photographs, NAIP imagery, oblique photographs, technical reports, and geologic maps. Along coastlines, bathymetry data are also important for locating the toes of landslides. The tabular data provide enough detail to track and filter on sizes of movements, types of movements, dates of movements, and material involved in the movements. Therefore, while my results were not identical to the DGER (2009) field-based inventory, they were within reason.

Two of the primary triggers for landslides in Washington State are increasing, which accelerates the need for the state to fund an inventory effort and the DGER to adopt a mapping protocol. Global warming is causing sea level rise in almost all parts of the state, and coastal bluffs are projected to erode more rapidly (Mauger et al., 2015). Additionally, the same intense, 24-hour rainstorms that led to failures in the winter of 1996/97 are also forecasted to increase, as is overall winter soil saturation which led to the movements

of the deep-seated landslides in 1998/99 (Mauger et al., 2015). This further supports my recommendation that the DGER should accept the DOGAMI protocol, with some adaptations:

1. The DGER uses an updated Varnes classification for landslide types and movement based on recent work of Hungr et al. (2014). This system is backward-compatible and uses geotechnical terms that environmental engineers and geologists understand and measure. It also allows for steep, coastal bluffs to be mapped as the category "soil slope deformation." This classification would be better suited to my map for landslides such as 'Squaxin Island 4pt2.' The DGER may want to add a separate column for Shannon and Wilson (2000) types of landslides, which are very useful when describing the glaciated shorelines of Washington that are not found along the Oregon coast. However, as the USGS shifts towards a common protocol for a comprehensive inventory of landslides throughout the United States, it will be important for Washington to remain with a version of the Varnes classification because it is common throughout the world and more useful than a locally developed classification system.
2. The DGER allows a GIS system to automate parts of the protocol such as calculating the slope (average slope within the landslide) and direction of movement (aspect tool). While the slope within a landslide is not the same as the failure of the original surface, the original surface is often modified or failing, too. If a more accurate slope is known or measured, that determination can be added by hand, but the accuracy of the profiles made in GIS is within a degree or two of the accuracy of the slope within the landslide area.
3. The DGER modifies the confidence system away from the DOGAMI points system. While the DOGAMI scoring system is supposed to be a calibration tool for mappers, a decision tree or a system that adds the pieces of evidence supporting the location and movement of the landslide (similar to what DGER (2009) used for their confidence level) is more meaningful and less ambiguous to others.
4. The DGER revises the terms for the age of landslide to use actual dates of recorded movement or best estimations of movement based on aerial photos or roughness dating (LaHusen et al., 2015). The terms historic, active, prehistoric, and ancient have different meanings to geologists and citizens, and it is better to be as precise as possible when communicating hazards and risks.
5. They DGER may want to keep the 38 data columns they developed in the 2009 project for times when they have additional funding or researchers because these additional data can develop future models. However, for the sake of providing a useful inventory of landslides for the citizens of Washington in a timely manner, they need to stick to the pertinent information outlined in the DOGAMI protocol, and complete these additional pieces of information only when they have additional time, mappers, or researchers.

My final recommendation is for Washington's legislators. Rather than relying on irregular grant money or occasional scientific studies, the state should set aside money to take oblique aerial photos on a regular basis. These photos help a range of users (personal communication with Hugh Shipman of the Department of Ecology, January 2016), and for projects like this one, taking photos at a consistent interval can show rates of change and help with risk calculations.

With limited fieldwork, the DOGAMI protocol provides a consistent and inexpensive means of capturing information on a GIS platform and it is already informing Oregon citizens and decision makers about landslide hazards (Burns and Madin, 2009). The citizens and decision makers of Washington deserve the same insight.

Epilogue: *Upon completing my inventory and writing this report, I am pleased to learn that the State of Washington passed senate bill (SB) 5088, which provides funding for the state Geological Survey (DGER) to apply best practices and obtain lidar for identifying hazards (including landslides) and share these data with the state and local governments (Office of Program Research, 2015). Furthermore, the DGER has assembled a team of mappers and they are going to use the DOGAMI protocol to create their inventory (personal conversation with Stephen Slaughter, 2016).*

Limitations

I did not go into the field to check the landslides; however, this was a purposeful limitation I implemented in order to check the accuracy at which I could map and make comparisons with the DGER (2009) inventory.

Another limitation is that I worked alone for much of this project, while the DGER worked in a team. Again, this approach was purposeful because this pushed me to learn and use tools within ArcGIS, and to think through the challenges of making a landslide inventory as an individual working professional would do. However, it also meant that I did not have as many discussions or dialogue about my observations and questions. Furthermore, it meant that I also worked slowly because I needed to solve ArcGIS problems on my own, and I could not divvy up the work.

Finally, this is my first landslide inventory effort. I do not have the same level of expertise as several of these previous researchers. Having different levels of expertise on a project is beneficial for several reasons, one being the passing on of skills and knowledge. Overall, what I lacked in experience I attempted to make up in documentation and thoroughness.

References

Baum, R.L., Coe, J.A., Godt, J.W., Harp, E.L., Reid, M.E., Savage, W.Z., Schulz, W.H., Brien, D.L., Chleborad, A.F., McKenna, J.P., and Michael, J.A., 2005, Regional landslide-hazard assessment for Seattle, Washington, USA: Landslides, v. 2, p. 266-279, doi: 10.1007/s10346-005-0023-y.

Booth, A.M., Roering, J.J., and Perron, J.T., 2009, Automated landslide mapping using spectral analysis and high-resolution topographic data: Puget Sound lowlands, Washington, and Portland Hills, Oregon: Geomorphology, v. 109, p. 132-147, doi:10.1016/j.geomorph.2009.02.027.

Booth, D.B., 1987, Timing and processes of deglaciation along the southern margin of the Cordilleran ice sheet, in Ruddiman, W.F., and Wright, H.E., *eds*., North America and adjacent oceans during the last deglaciation: Boulder, Colorado, Geological Society of America, the Geology of North America, v.K-3, p. 71-90.

Booth, D.B., 1994, Glaciofluvial infilling and scour of the Puget Lowland, Washington, during ice-sheet glaciation: Geology, v. 22, p. 695-698.

Borden, R.K., and Troost, K.G., 2001, Late Pleistocene stratigraphy in the south-central Puget Lowland, Pierce County, Washington: Washington Division of Geology and Earth Resources Report of Investigations 33, 33 p.

Burns, W. J., 2007, Comparison of remote sensing datasets for the establishment of a landslide mapping protocol in Oregon, *in Proceedings*, AEG Special Publication 23, Vail, Colorado Conference Presentations, 1st North American Landslide Conference, p. 335-345.

Burns, W.J., and Madin, I.P., 2009, Protocol for inventory mapping of landslide deposits from light detection and ranging (LIDAR) imagery: Oregon Department of Geology and Mineral Industries, Special paper 42, 26 p.

Clement, C.R., Pratt, T.L., Holmes, M.L., and Sherrod, B.L., 2010, Growth folding and shallow faults in the southern Puget Lowland, Washington State: Bulletin of the Seismological Society of America, v. 100(4), p. 1710-1723.

Cruden, D.M., and Varnes, D.J., 1996, Landslide types and processes, *in* Turner, A.K., and Schuster, R.L., eds., Landslides—Investigation and mitigation: Washington, D.C., Transportation Research Board Special Report 247, p. 36-75.

Duncan, R.A., 1982, A captured island chain in the Coast Range of Oregon and Washington: Journal of Geophysical Research, v. 87, n. B13, p. 10,827-10,837.

GeoEngineers, 1999, Phase I – Reconnaissance evaluation, and Phase II – Geotechnical study, Carlyon Beach/Hunter Point Landslide, prepared for Thurston County Development Services, Olympia, Washington.

Gerstel, W.J., Brunengo, M.J., Lingley, W.S., Logan, R.L., Shipman, H., and Walsh, T.J., 1997, Puget Sound bluffs: The where, why, and when of landslides following the Holiday 1996/97 storms: Washington Geology, v. 25 (1), p. 17-31.

Guzzetti, F., 2005, Landslide hazard and risk assessment [PhD. Dissertation]: Bonn, Rheinischen Friedrich-Wilhelms-Univestität Bonn, 373 p.

Guzzetti, F., Mondini, A.C., Cardinali, M., Fiorucci, F., Santangelo, M., and Chang, K.T., 2012, Landslide inventory maps: New tools for an old problem: Earth-Science Reviews, v. 112, p. 42-66.

Haugerud, R.A., Harding, D.J., Johnson, S.Y., Harless, J.L., and Weaver, C.S., 2003, High-resolution lidar topography of the Puget Lowland, Washington: GSA Today v. 13(6) , p. 4-10.

Hungr, O., Leroueil, S., Picarelli, L., 2014, The Varnes classification of landslide types, an update: Landslides, v. 11, p. 167-194, doi: 10.1007/s10346-013-0436-y.

Keaton, J.R., Wartman, J., Anderson, S., Benoît, J., deLaChapelle, J., Gilbert, R., and Montgomery, D.R., 2014, The 22 March 2014 Oso Landslide, Snohomish County, Washington: GEER Association Report No. GEER-036.

Kirschbaum, D.B., Alder, R., Hong, Y., Hill, S., and Lerner-Lam, A., 2009, A global landslide catalog for hazard applications: method, results, and limitations: National Hazards, v. 52, p. 561-575, doi: 10.1007/s11069-009-9401-4.

Lasmanis, Raymond, 2001, Surviving the Nisqually Earthquake: Washington Geology, v. 28 (3), p. 3-19.

LaHusen, S.R., Duvall, A.R., Booth, A.M., and Montgomery, D.R., 2015, Surface roughness dating of long-runout landslides near Oso, Washington (USA), reveals persistent postglacial hillslope instability: Geology, v. 44(2), p. 111-114, doi: 10.1130/G37267.1.

Logan, R.L., Polenz, M., Walsh, T.J., and Schasse, H.W., 2003, Geologic map of the Squaxin Island 7.5-minute quadrangle, Mason and Thurston Counties, Washington: Washington Division of Geology and Earth Resources Open-File Report 2003-23, scale 1:24,000.

Logan, R.L., and Walsh, T.J., 2004, Geologic map of the Summit Lake 7.5-minute quadrangle, Thurston and Mason Counties, Washington: Washington Division of Geology and Earth Resources Open-File Report 2004-10, scale 1:24,000.

Lombardo, K., Boggs, J., Boudreau, J., Chiles, P., Erikson, J., Gerstel, W., Montgomery, D., Shipman, L., Radcliff-Sinclair, R., Strachan, S., Sugimura, D., and Trimm, B., 2014, SR 530 Landslide commission final report: State of Washington Open-File Report (paper copy, 49 p.).

Malone, S., Crosson, B., Creager, K., Qamar, T., Thomas, G., Ludwin, R., Troost, K., Booth, D., and Haugerud, R., 2001, Preliminary report on the M_W=6.8 Nisqually, Washington earthquake of 28 February 2001: Seismological Research Letters, v.72 (3), p. 352-361.

Mauger, G.S., Casols, J.H., Morgan, H.A., Strauch, R.L., Jones, B., Curry, B., Busch Isaksen, T.M., Binder L.W., Krosby, M.B., and Snover, A.K., 2015, State of Knowledge: Climate Change in Puget Sound: Report prepared for the Puget Sound Partnership and the National Oceanic and Atmospheric Administration, Climate Impacts Group, University of Washington, Seattle, p.28, doi: 107915/CIG93777D.

McKenna, J.P., Lidke, D.J., Coe, J.A., 2008, Landslides mapped from LIDAR imagery, Kitsap County, Washington: U.S. Geological Survey Open-File Report 2007-1292, 81 p.

Office of Program Research, 2015, Final summary of the legislation passed by the Washington State Legislature: Office of Program Research Washington, House of Representatives, Olympia, 104 p.

Pratt, T.L., Johnson, S., Potter, C., Stephenson, W., and Finn, C., 1997, Seismic reflection images beneath Puget Sound, western Washington State: The Puget Lowland thrust sheet hypothesis: Journal of Geophysical Research, v. 102 (B12), p. 27,469-27,489.

Ryan, A., 2015, Partnership shows lidar's practical use, potential in Oregon: LiDAR Magazine, v. 5 (5), p. 36-40.

Sarikhan, I.Y., Stanton, K.D., Contreras, T.A., Polenz, M., Powell, J., Walsh, T.J., and Logan, R.L., 2008, Landslide reconnaissance following the storm event of December 1-3, 2007, in western Washington: Washington Division of Geology and Earth Resources Open-File Report 2008-5, 16 p.

Schasse, H.W., Logan, R.L., Polenz, M., and Walsh, T.J., 2003, Geologic map of the Shelton 7.5-minute quadrangle, Mason and Thurston Counties, Washington: Washington Division of Geology and Earth Resources Open-File Report 2003-24, scale 1:24,000.

Schulz, W.H., 2007, Landslide susceptibility revealed by LIDAR imagery and historical records, Seattle, Washington: Engineering Geology, v. 89, P.67-87.

Shannon and Wilson, Inc., 1999, Phase 2 Geotechnical Report: Sunrise Beach Road NW landslide, prepared for Thurston County Department of Roads and Transportation Services, Olympia.

Shannon and Wilson, Inc., 2000, Seattle Landslide Study, Seattle Public Utilities, v. 1 and v. 2, 164 p. and 34p.

Shipman, H., 2001, Coastal landsliding on Puget Sound: A review of landslides occurring between 1996 and 1999, Publication #01-06-019, Shorelands and Environmental Assistance Program, Washington Department of Ecology, Olympia, 86 p.

Slaughter, S., 2015, Landslide inventories in Washington State: the past, present, and future: http://c.ymcdn.com/sites/www.aegweb.org/resource/resmgr/Landslides/10AEG_2015_Slaughter.pdf (accessed April 2016).

Thurston County Development Services Department, 2008, Thurston County comprehensive plan: Olympia, Washington, http://www.co.thurston.wa.us/planning/comp_plan/comp_plan_document.htm (accessed April 2016).

Thurston Geodata Center, 1986, County boarder: Thurston County, Washington, Thurston Geodata Center, www.geodata.org (accessed April 2016).

Thurston Geodata Center, 2012, Thruston County lidar, hydro-enforced DEM v.01: Olympia, Washington, Thurston Geodata Center, http://pugetsoundlidar.ess.washington.edu/lidardata/restricted/nonpslc/thurston2011/Thurston_LiDAR_DEM_Metadata_.html (accessed April 2016).

Thurston Geodata Center, Stormwater Department, and Thurston County Current Planning, 1993, Basins and watersheds: Thurston County, Washington, Thurston Geodata Center, www.geodata.org (accessed April 2016).

Troost, K.G., and Booth, D.B., 2008, Geology of Seattle and the Seattle area, Washington, *in* Baum, R.L., Godt, J.W., and Highland, L.M., eds., Landslides and Engineering Geology of the Seattle,

Washington, area: Geological Society of America Review in Engineering Geology, v. XX, p. 1-35, doi: 10.1130/2008.4020(01).

Varnes, D.J., 1978, Slope movement types and processes, *in* Schuster, R.L., and Krizek, R.J., eds., Landslides—analysis and control: Washington, D.C., Transportation Research Board Special Report 176, p. 11-33.

Walsh, T.J., Logan, R.L., Schasse, H.W., and Polenz, M., 2003, Geologic map of the Tumwater 7.5-minute quadrangle, Thurston County, Washington: Washington Division of Geology and Earth Resources Open-File Report 2003-25, scale 1:24,000.

Washington State Department of Ecology, 1994, USGS 7.5' quadrangle boundaries (1:24,000 scale): Olympia, Washington, Washington State Department of Ecology http://www.ecy.wa.gov/services/gis/data/data.htm#q) (accessed 2016).

Washington State Department of Ecology, 1994, Washington Base Map: Olympia, Washington, Washington State Department of Ecology http://www.ecy.wa.gov/services/gis/data/data.htm#w (accessed 2016).

Washington Division of Geology and Earth Resources (DGER), 2009, Marine shore landslides and landforms of Thurston County, Washington: Washington DGER ESRI shapefiles, metadata for the shapefiles, two layer files for ArcGIS, four supporting Microsoft Word and Excel documents, and README.doc.

Washington Division of Geology and Earth Resources (DGER), 2014, Surface geology, 1:24,000--GIS data, June 2014: Washington Division of Geology and Earth Resources Digital Data Series DS-10, version 1.0., http://www.dnr.wa.gov/publications/ger_portal_surface_geology_24k.zip (accessed 2015).

Washington Division of Geology and Earth Resources (DGER), 2015, Significant deep-seated landslides in Washington State—1984 to 2014: http://file.dnr.wa.gov/publications/ger_list_large_landslides.pdf (accessed 2016).

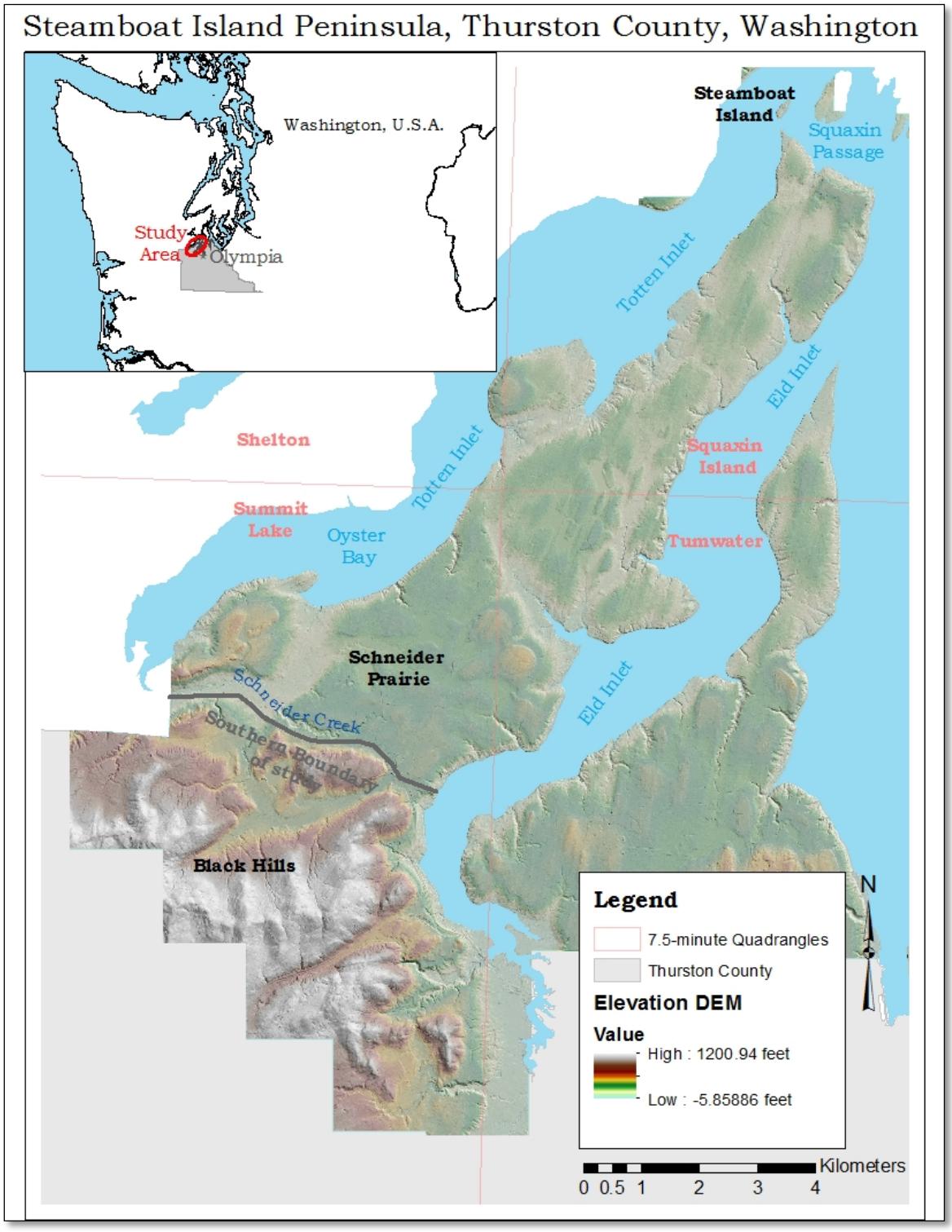

Figure 1: Location Map

Inset map shows the study area in Thurston County, Washington, while the larger map shows Steamboat Island Peninsula and the southern extent of the study area (Thurston Geodata Center, 2012; Washington Department of Ecology, 1994).

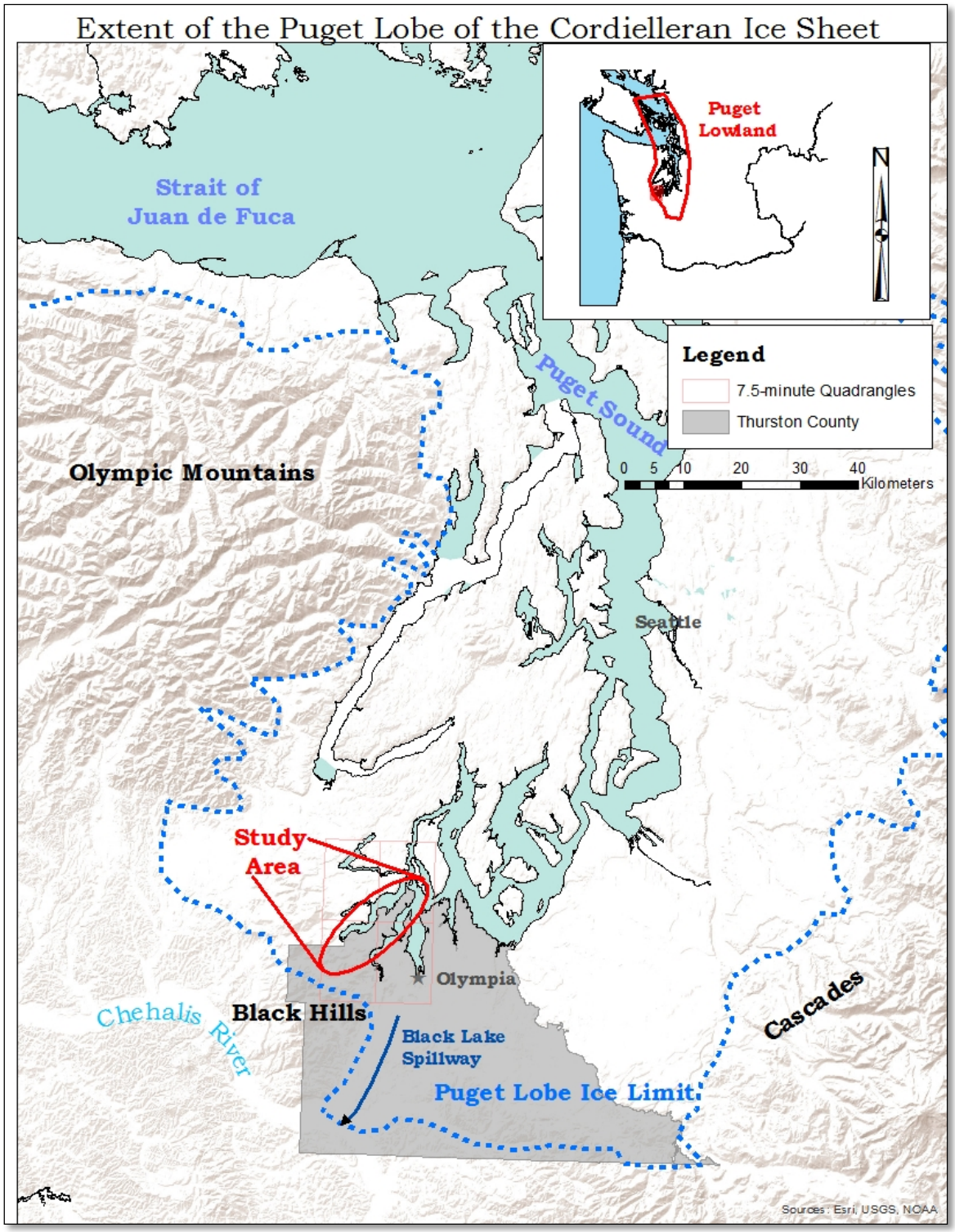

Figure 2: Location of the Puget Lowland and the extent of the Puget Lobe

Larger map shows the study area in relation to the larger Puget Lowland, which is outlined in the inset map of Washington State (Thurston Geodata Center, 1986; Thurston Geodata Center et al., 1993; Washington Department of Ecology, 1994). The Puget Lobe ice limit and Black Lake Spillway are from Troost and Booth (2008).

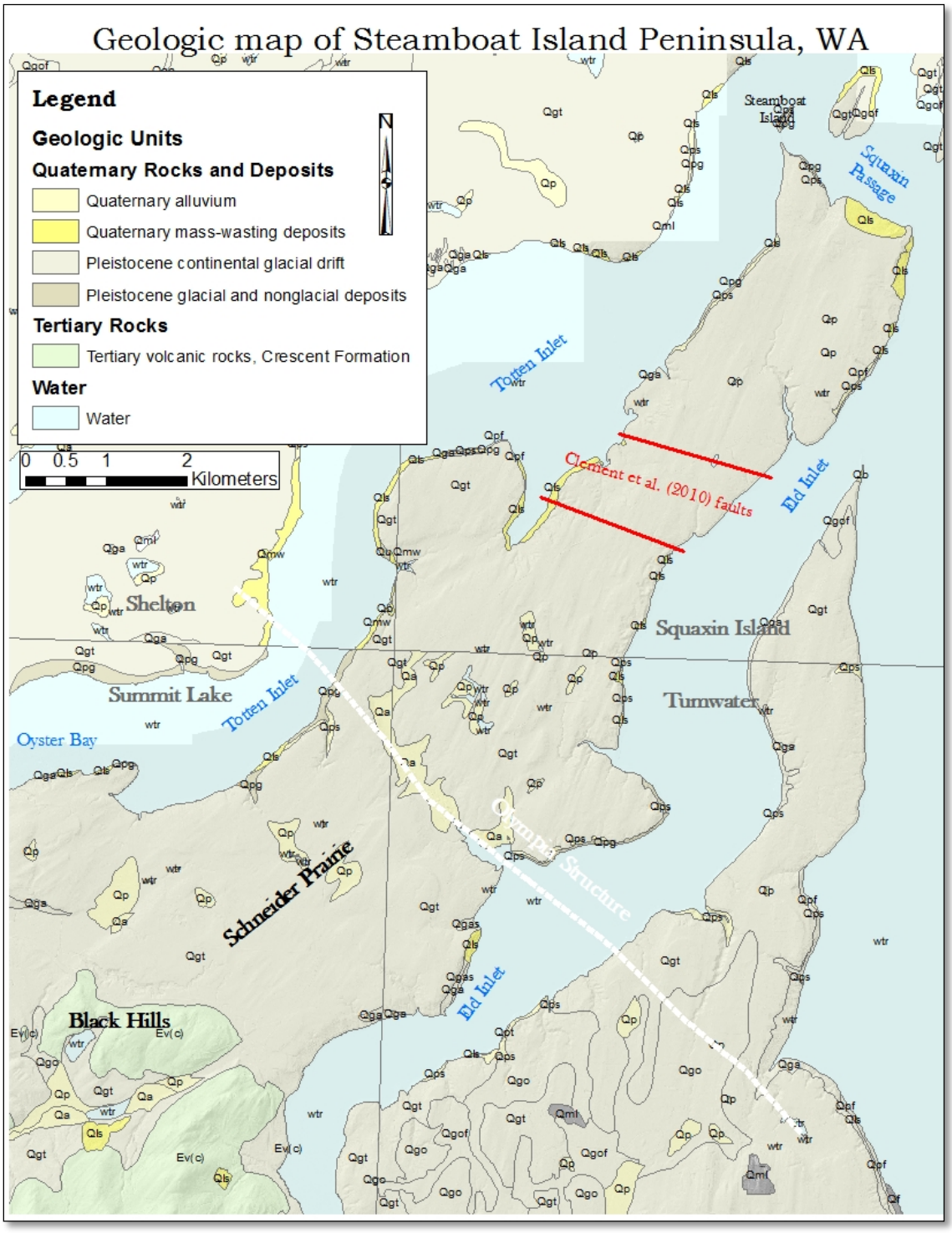

Figure 3: Geologic Map of Steamboat Island Peninsula

The geologic map of the study area, Steamboat Island Peninsula, Thurston County, which is shown at a smaller scale in Figure 2 (DGER, 2014) (Refer to Table 1 for description of geologic symbols). The Olympia Structure is interpreted as either a monocline or a "thin-skinned" thrust sheet (Pratt et al., 1997; Logan and Walsh, 2004; Clement et al., 2010). The red lines are interpreted by Clement et al. (2010) as late Pleistocene or early Holocene faults.

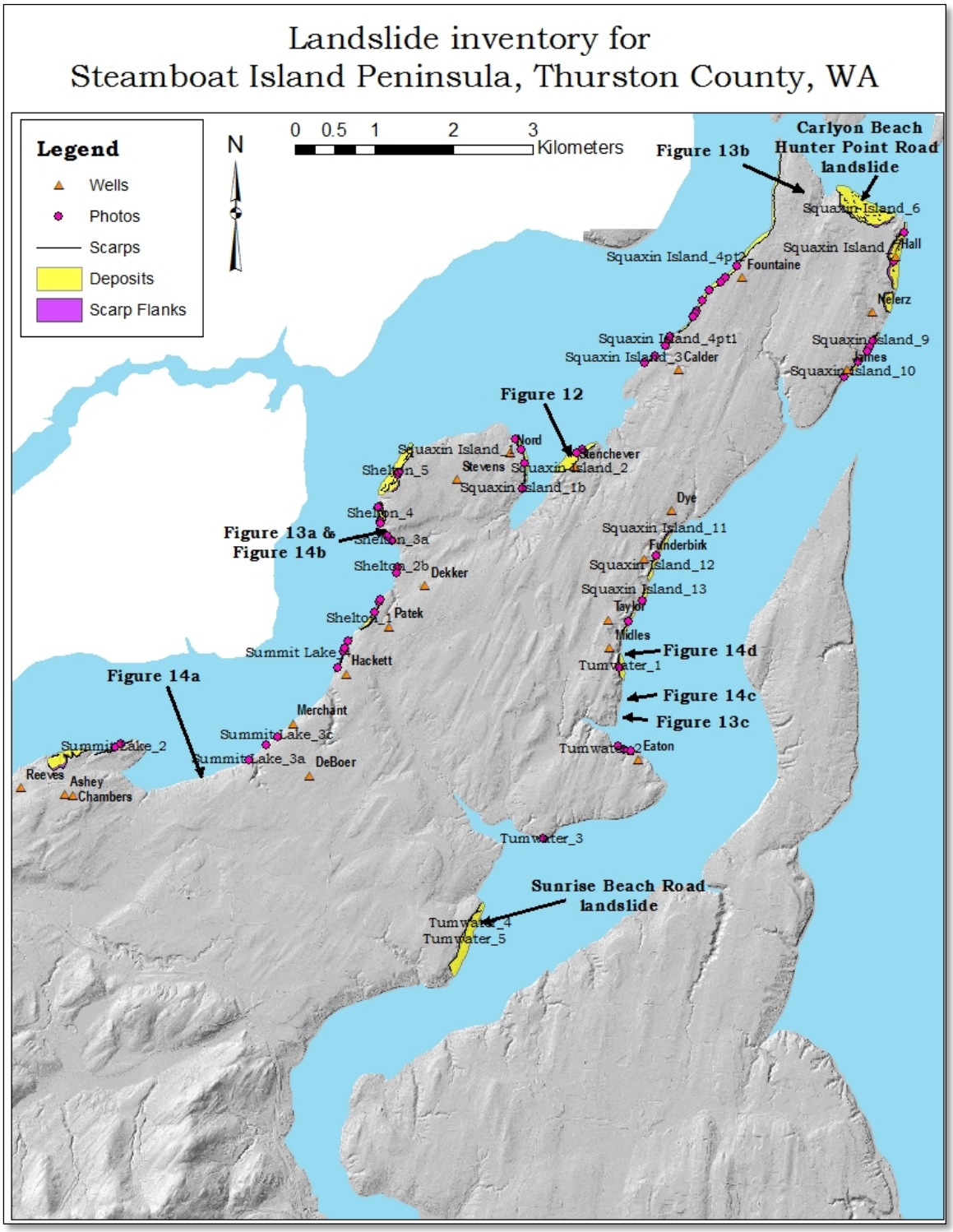

Figure 4: Landslide Inventory for Steamboat Island Peninsula
The complete landslide inventory map I created using the DOGAMI protocol (Burns and Madin, 2009). All total, I found 36 landslide deposits (yellow) and 48 recent movements (pink dots). I used the nearest, detailed well logs from the Department of Ecology (orange diamonds) to determine the geology of the landslides. (Hillshade with 315-degree illumination azimuth created from DEM – Thurston Geodata Center, 2012).

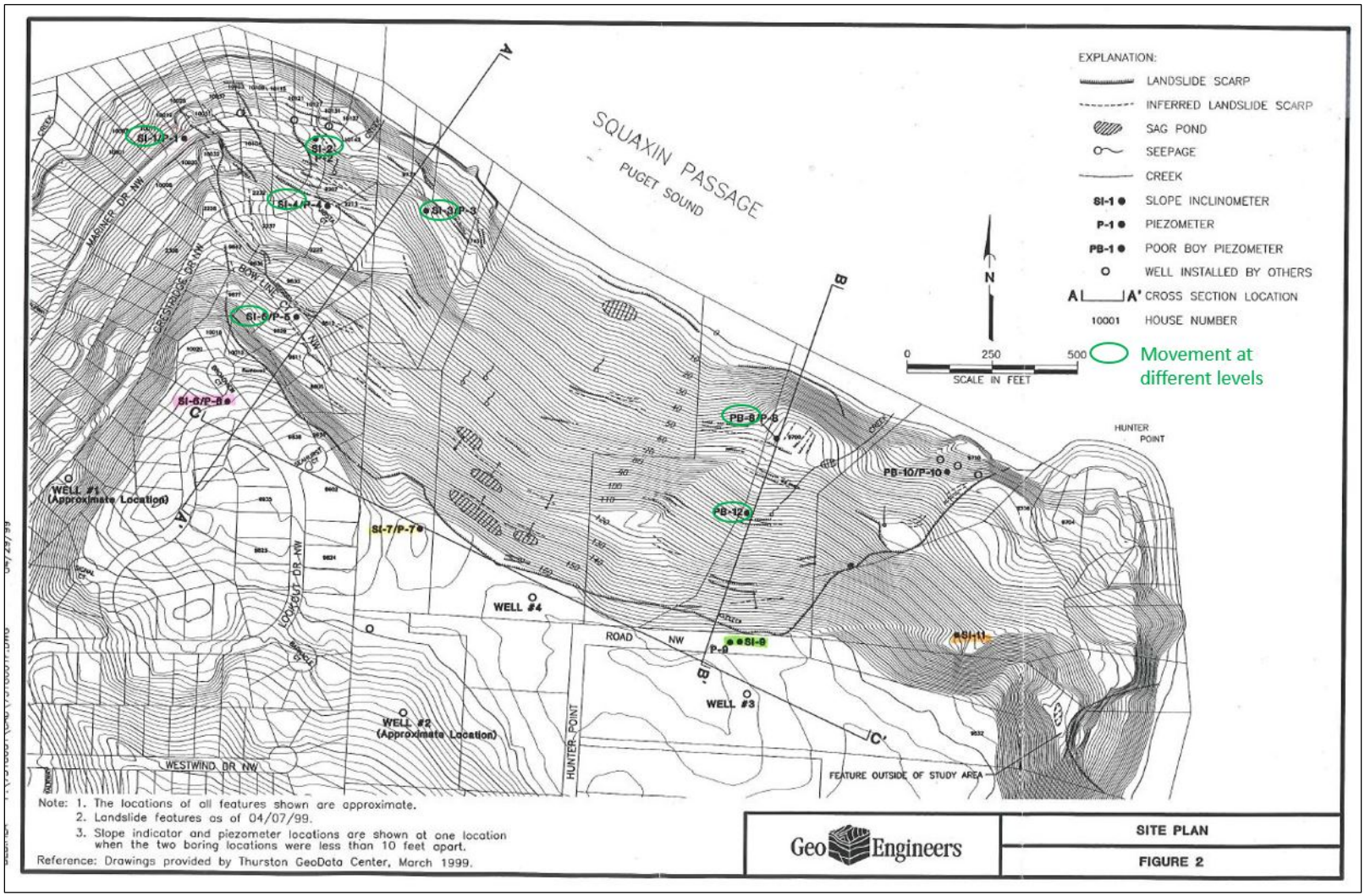

Figure 5: GeoEngineers Site Map of Carlyon Beach/ Hunter Point Road landslide
The site map of the Carlyon Beach/ Hunter Point Road landslide as mapped by GeoEngineers (1999). I used this map to mark the head and flank scarps for my landslide inventory.

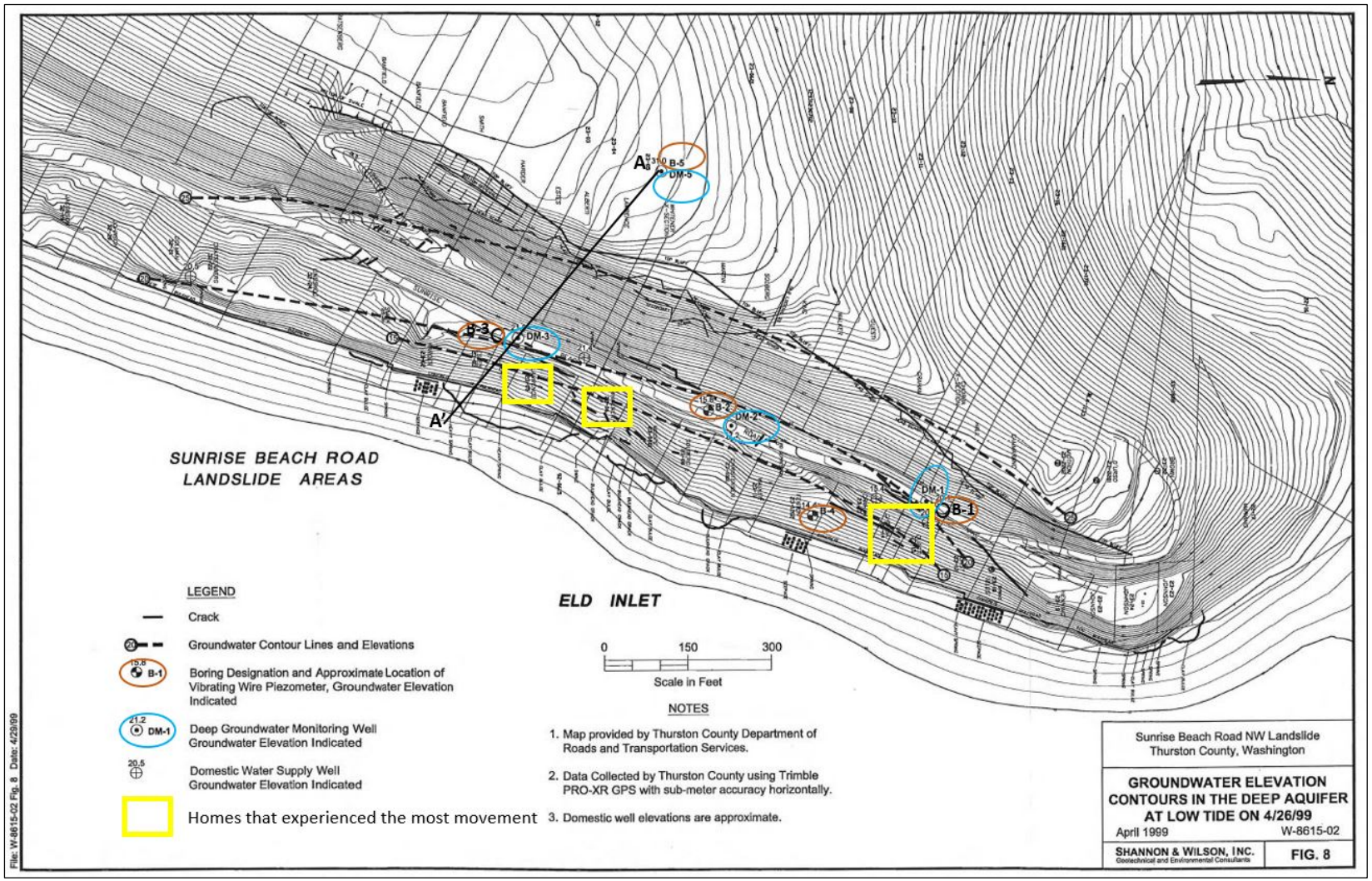

Figure 6: Shannon and Wilson site map of Sunrise Beach Road landslide
The Sunrise Beach Road landslide site map as surveyed by Shannon and Wilson (1999). Note the brown ovals, which show the locations of the inclinometers that moved during the 2001 Nisqually Earthquake. Also note the locations of the homes most damaged by the landslide.

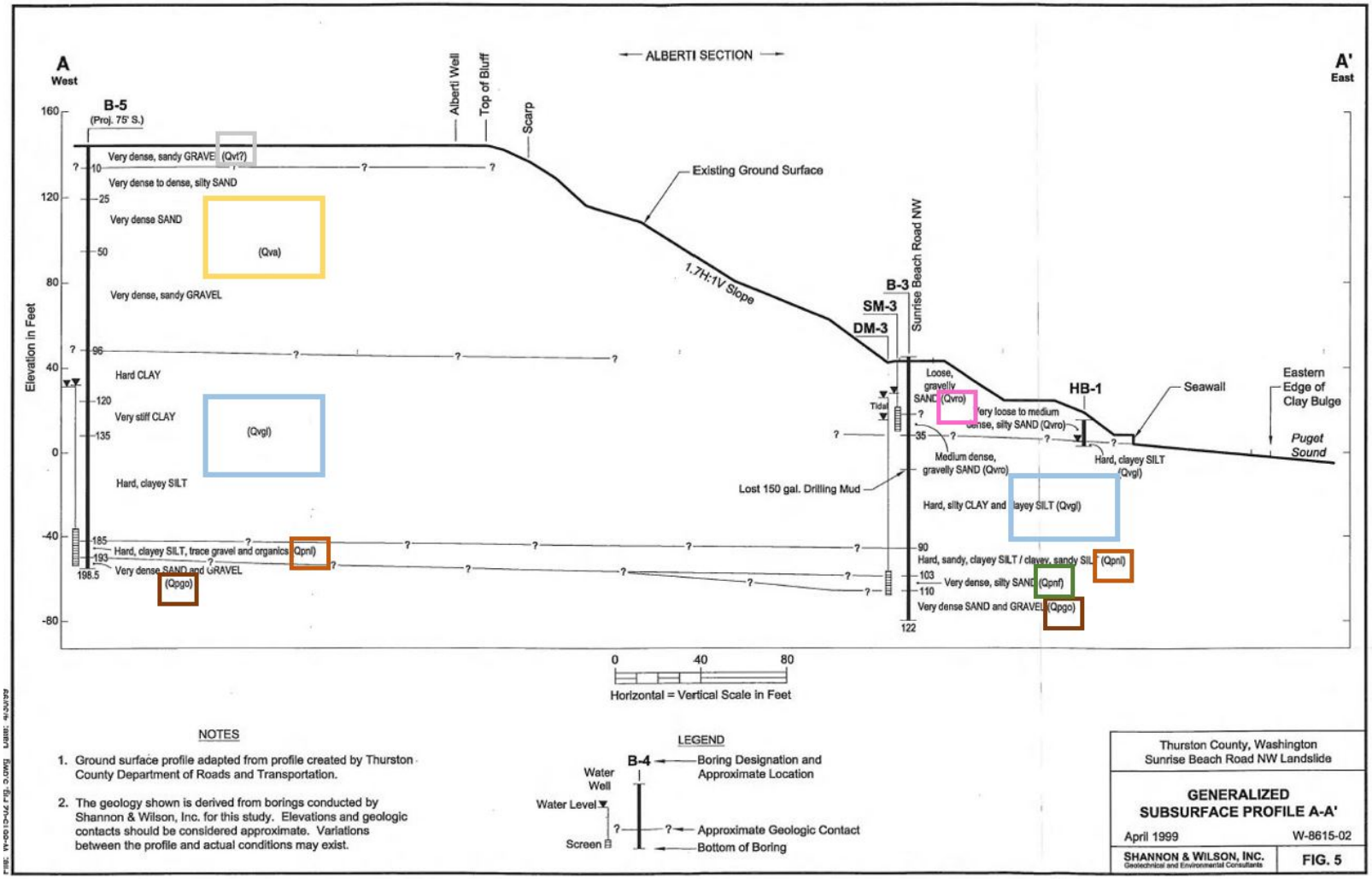

Figure 7: Cross section of Sunrise Beach Road landslide

The stratigraphy of Sunrise Beach Road landslide as interpreted by Shannon and Wilson (1999) from bore logs (B-5 and B-3) and hand bore logs (HB-1). Note that the geology on the east and the west sides of the road differs.

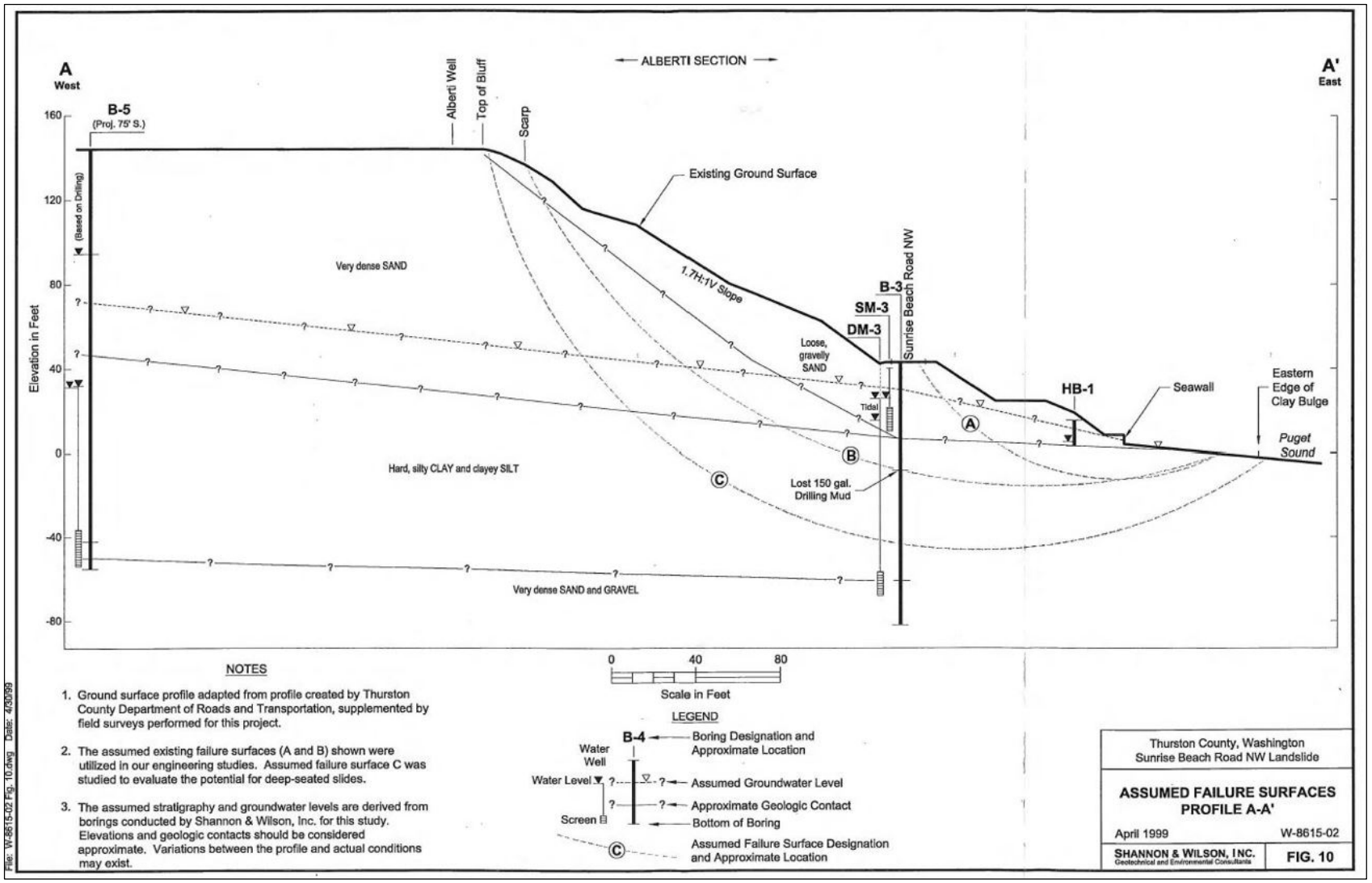

Figure 8: Cross section showing rotational depth of Sunrise Beach Road landslide

Shannon and Wilson (1999) determined that the reactivation of the Sunrise Beach Road landslide occurred along level B, where 150 gallons of drilling mud disappeared. The larger complex probably moved along level C in the past (Shannon and Wilson, 1999).

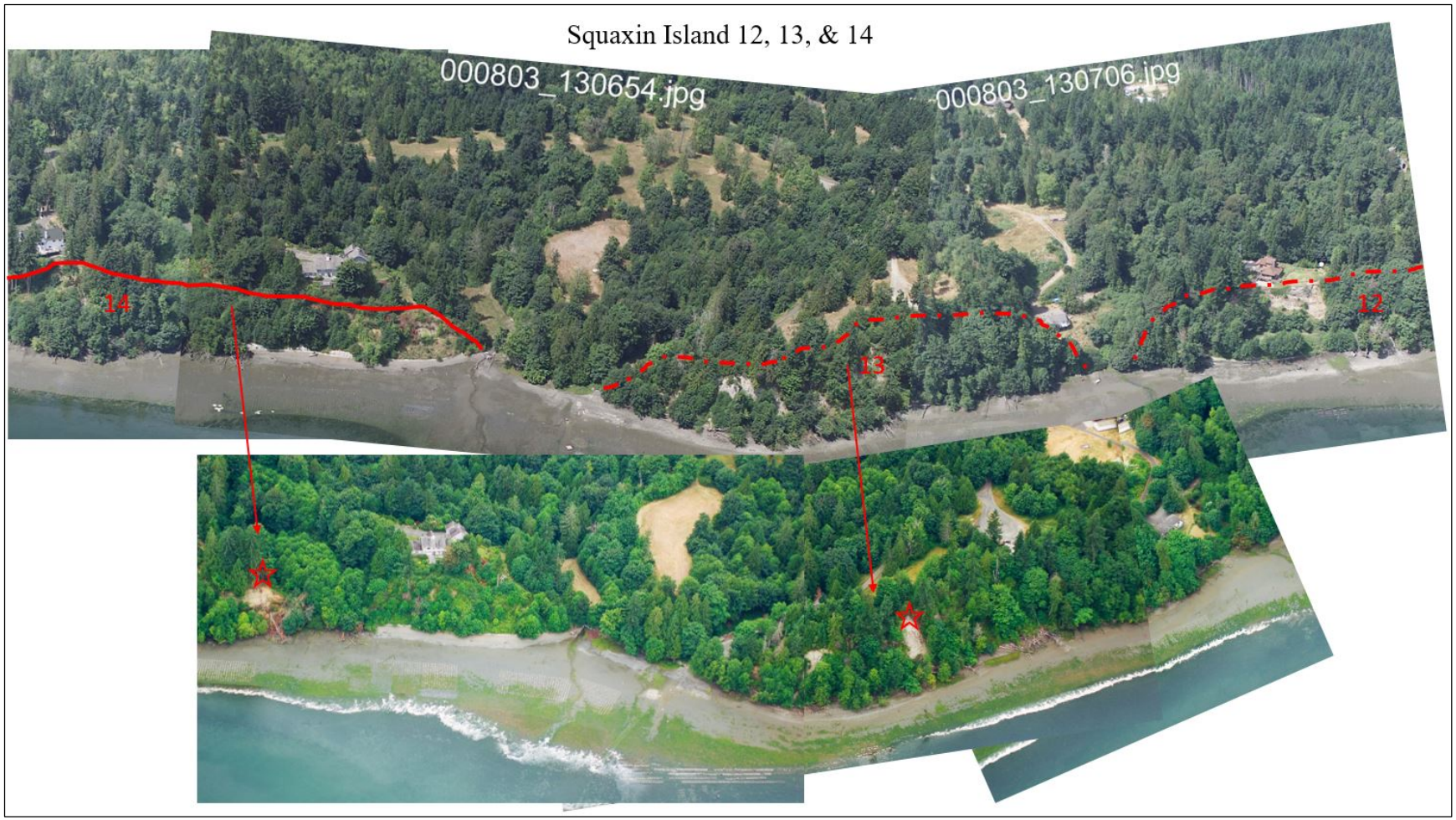

Figure 9: Photos showing movement of Squaxin Island 12, 13, and 14 landslides
An example of downloaded photos from the Department of Ecology's "Coastal Atlas Map: Shoreline Photos". I used these photos to aid in finding landslides (https://fortress.wa.gov/ecy/coastalatlas/tools/Map.aspx). The upper photos are from 2000 and the lower series are from 2006. I created similar imagery for each of my landslides.

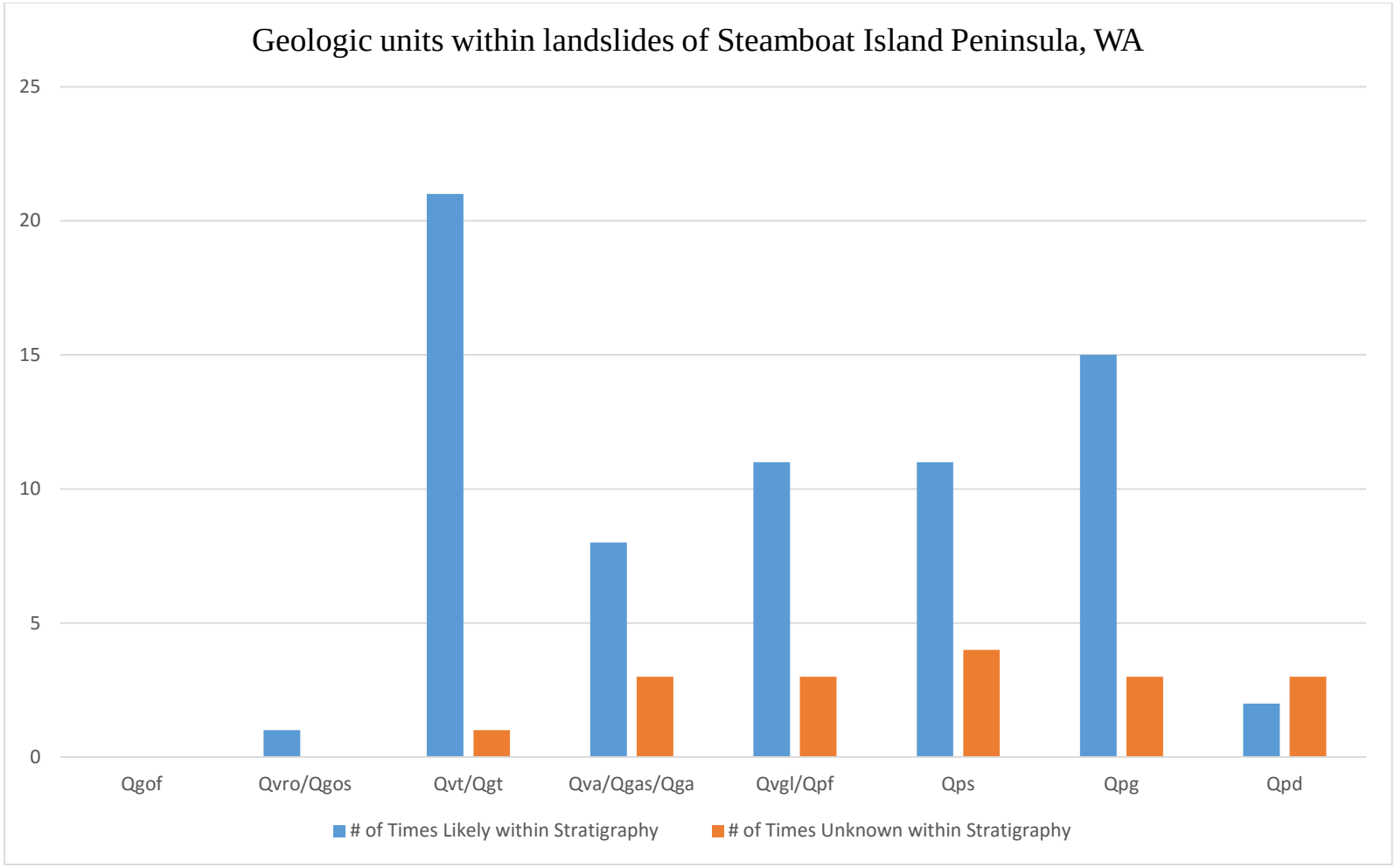

Figure 10: Bar graph showing the glacial sediments involved in 36 landslides
Bar graph showing the glacial and interglacial sediments involved in the 36 landslides identified in this study. "Times Likely within Stratigraphy" indicates sediments that are likely a part of the landslide deposit; "Times Unknown within Stratigraphy" means that this unit may be a part of the landslide deposit, but it is difficult to tell from the available maps and well logs. As it is a thin layer draped across the landscape, the Vashon glacial till (Qvt/Qgt) is likely a part of most of the landslides. The advanced outwash (Qva/Qgas/Qga), glacial lacustrine (Qvgl/Qpf), and pre-Vashon sands and gravels (Qps and Qpg) are thicker units below the till.

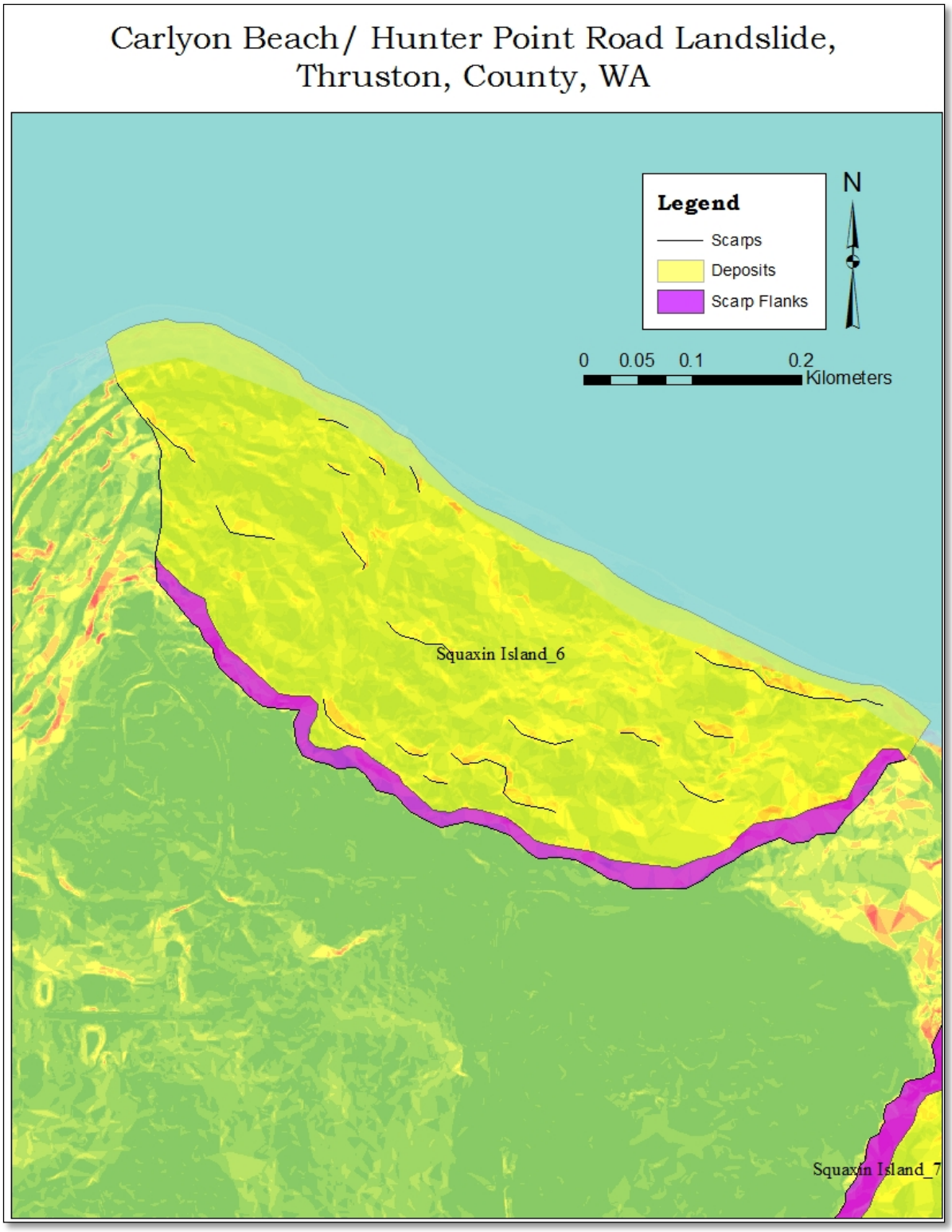

Figure 11: Internal scarps digitized on Carlyon Beach/ Hunter Point Road landslide
Internal scarps within the Carlyon Beach/ Hunter Point Road landslide (Squaxin Island 6) are challenging to digitize. The algorithm used to "remove" trees creates facets, which do not necessarily represent the bare earth.

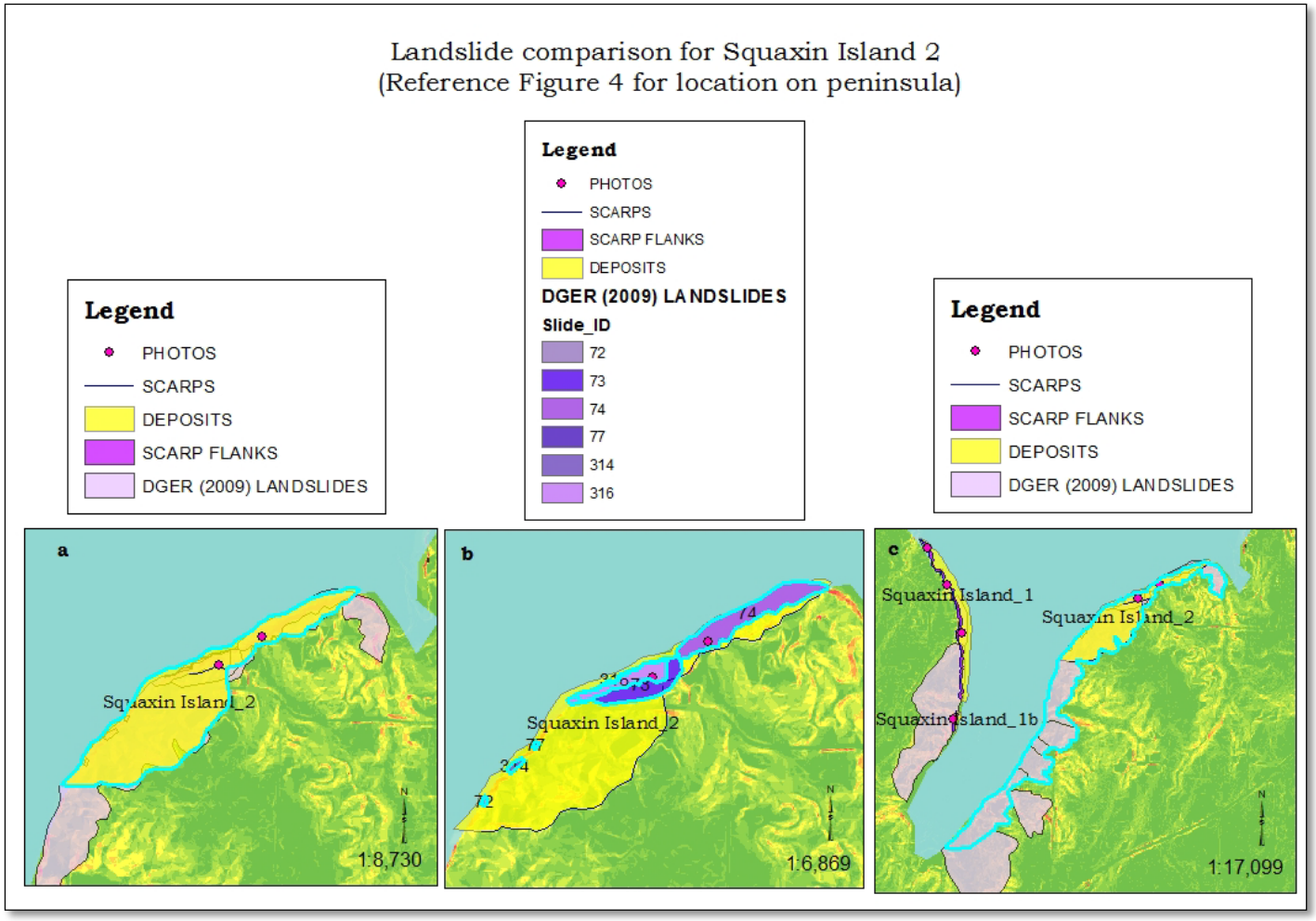

Figure 12: Comparison of landslide complexes
Inset a: The landslide I classified as a complex (Squaxin Island 2—see Figure 4) is shown highlighted in cyan. **Inset b**: Within my Squaxin Island 2, the DGER (2009) found six smaller landslides (cyan). **Inset c**: Additionally, the DGER (2009) also mapped my Squaxin Island 2 within a larger complex. This is why our numbers differ, and the discrepancy forced me to evaluate each slide individually.

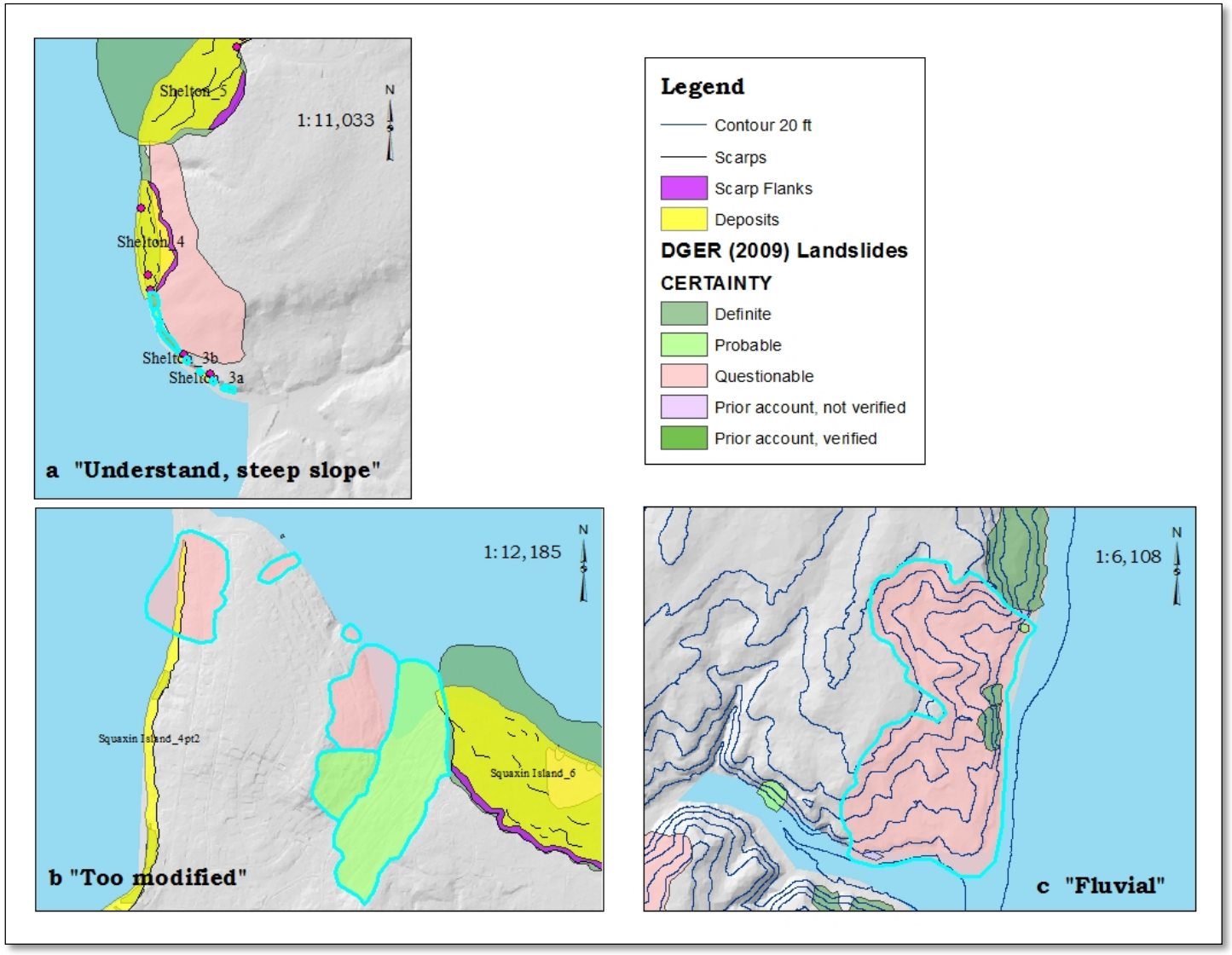

Figure 13: Evaluation of landslides not mapped in this study but identified by DGER (2009)
Examples of the classification I used to understand the difference between my landslide map and the DGER (2009) landslide map.

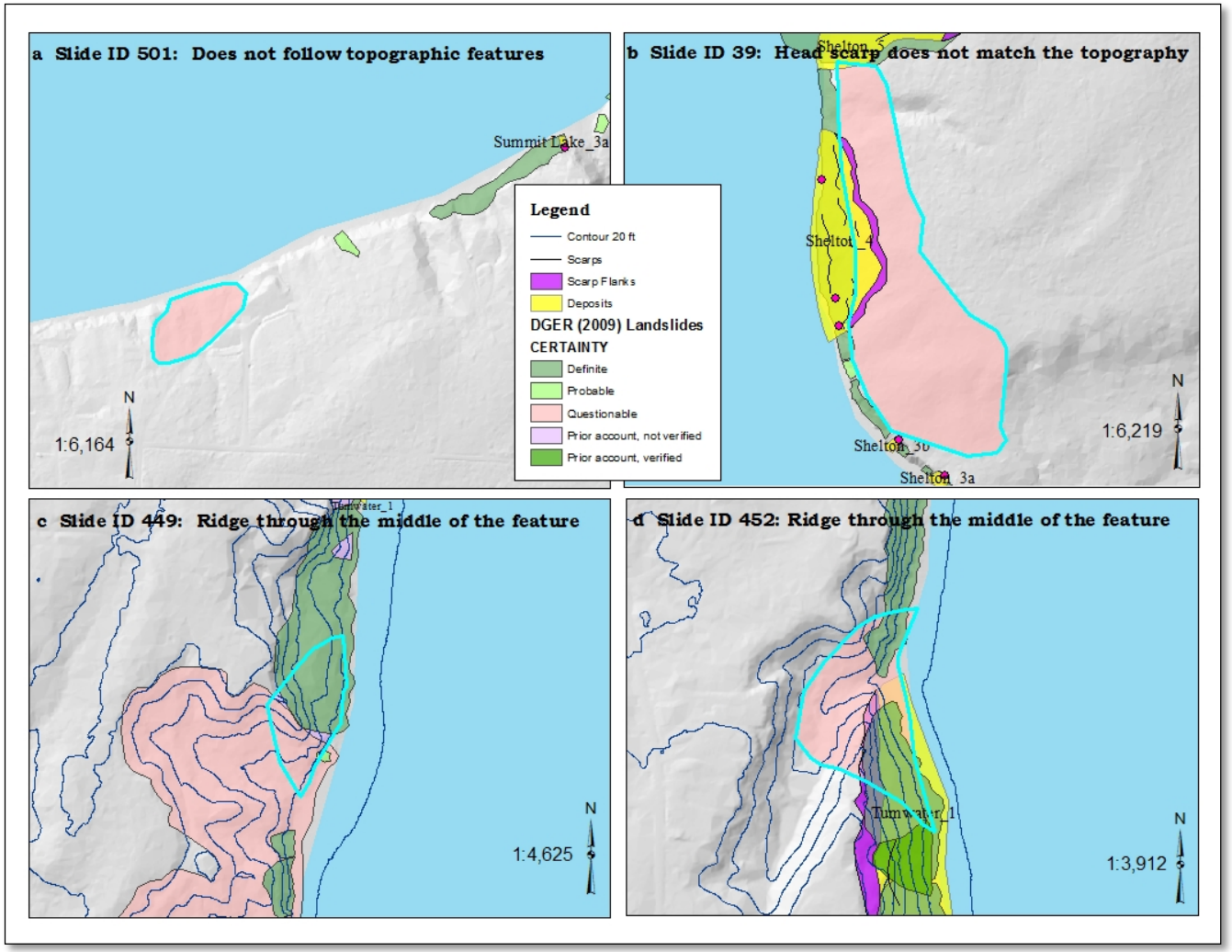

Figure 14: Landslides digitized as part of DGER (2009) inventory that I marked as "Disagree"

Four landslides the DGER (2009) included in their inventory along Steamboat Island Peninsula, and my justification for disagreeing with classifying these polygons as landslide movements.

Table 1: Summary of the sediments found on Steamboat Island Peninsula, and the symbols used to represent these sediments.

7.5-minute Quadrangle	Mapping Authors	Pleistocene Glacial Deposits and Symbols
Squaxin Island	Logan, Polenz, Walsh & Schasse, 2003	**Qgof – Latest Vashon fine-grained sediments**; lacustrine clay and/or fine sandy silt; maximum thickness in area 3m (10ft) **Qgos – Latest Vashon recessional sand and minor silt**; noncohesive, fine- to medium-grained sand with minor silt; maximum thickness in area 30m (100ft) **Qgt – Vashon till**; Unsorted and highly compacted mixture of clay, silt, sand, and gravel; maximum thickness in area 9m (30ft) **Qga & Qgas – Vashon advance Outwash**; sand and gravel and lacustrine clay, silt and sand of northern and Olympic Range source **Qpf – Pre-Vashon glaciolacustrine deposits** – laminated clayey and/or fine sandy silt with limited organic matter; maximum thickness in area <3m (10ft) **Qps – Pre-Vashon sandy deposits**; thin- to thick-bedded sand interbedded with silt and minor peat, diatomite, and gravel; two radiocarbon dates from this sand and silt put at 33,220 ±300 yr B.P. to 38,060 ±620 yr B.P. **Qpg – Pre-Vashon gravel**; gravel and sand from northern provenance; under or interbedded with Qps.
Shelton	Schasse, Logan, Polenz, and Walsh, 2003	**Qgof – Latest Vashon fine-grained sediments** **Qgo – Vashon recessional outwash**; difficult to discern from Qga in some areas **Qgt – Vashon till** **Qga – Vashon advance outwash** **Qpf – Pre-Vashon glaciolacustrine deposits;** peaty silt at Hammersley Inlet (north of mapping area) produced ^{14}C age of >42,810 yr B.P. **Qps – Pre-Vashon sandy deposits** **Qpg; Qpg$_o$ – Pre-Vashon gravel**; inferred to be of glacial origin because of size of gravel and northern origin of these gravels; **Qgo** has Olympic-source basalt and sandstone clasts **Qpd – Pre-Vashon drift**; blue-gray glaciolacustrine beds
Summit Lake	Logan & Walsh, 2004	**Qgos – Latest Vashon recessional sand and minor silt** **Qgo – Vashon recessional outwash** **Qgt – Vashon till** **Qga & Qgas – Vashon advance Outwash**; maximum thickness 30m (100ft); locally called Colvos Sand but generally correlated with Esperance Sand **Qpf – Pre-Vashon glaciolacustrine deposits**; locally maximum thickness 30m (100ft) **Qps – Pre-Vashon sandy deposits** **Qpg – Pre-Vashon gravel** **Qpd – Pre-Vashon drift**; weathering rinds on basaltic stones 1 to 2mm thick
Tumwater	Walsh, Logan, Schasse, and Polenz, 2003	**Qgof – Latest Vashon fine-grained sediments** **Qgos – Latest Vashon recessional sand and minor silt;** under Capitol Lake reaches a maximum thickness of 130m (420ft) **Qgo – Vashon recessional outwash** **Qgt – Vashon till** **Qga & Qgas – Vashon advance Outwash**; maximum thickness 30m (100ft) **Qpf – Pre-Vashon glaciolacustrine deposits**; locally maximum thickness 30m (100ft) **Qps – Pre-Vashon sandy deposits** **Qpg – Pre-Vashon gravel**

Table 2: Inclinometer Data for Sunrise Beach Road landslide

Inclinometer data collected by Thurston County as part of their long-term monitoring plan; Figure 5 shows the locations of B-1i, B-2i, and B-3i (personal communication from Mark P. Biever to Thurston County Roads and Transportation, 2000).

Inclinometer ID	**B-1i**		**B-2i**	**B-3i**	
Initialization Date	2/27/2001		11/13/2000	3/7/2001	
Reading Dates	Zone 1 18ft Cumulative Deflection	Zone 2 65ft Cumulative Deflection	Zone 1 34ft Cumulative Deflection	Zone 1 35ft Cumulative Deflection	Zone 2 52ft Cumulative Deflection
2/27/2001	0.00”	0.00”	0.00”	0.00”	0.00”
3/1/2001	0.11”	0.04”	0.03”	0.08”	0.02”
3/7/2001	0.12”	0.05”	0.05”	0.09”	0.03”
6/18/2001	0.13”	0.05”	0.06”	0.09”	0.03”
12/9/2002	0.13”	0.05”	0.06”	0.09”	0.03”
6/16/2004	0.13”	0.05”	0.06”	0.09”	0.03”
2/24/2005	0.13”	0.05”	0.06”	0.09”	0.03”
Total Measured Deflection	**0.13”**	**0.05”**	**0.06**”	**0.09**”	**0.03**”

Table 3: Data types, sources, and resolution

Summary of the data types used for completing this project, their source, and resolution / scale.

Data Type	Source	Resolution/Scale
2011 Lidar; .adf files	Thurston Geodata Center	1m, hydro enforced DEM
2009, 2011, 2013 Orthorectified NAIP; .tif files	WAGDA	1-m, 4-band
1965 black-and-white aerial photo series	DGER	1:12,000
1971 high-elevation black-and-white aerial photo series	DGER	1:66,000
1972 high-elevation black-and-white aerial photo series	DGER	1:66,000
1976 color aerial photo series	DGER	1:24,000
2003 color aerial photo series	DGER	1:12,000
1997, 1992-97, 2000, and 2006 Oblique shoreline photos; .jpg	WA Dept. of Ecology	None
7.5-minute quadrangle of Summit Lake; .pdf	Logan & Walsh, 2004	1:24,000
7.5-minute quadrangle of Shelton; .pdf	Schasse et al., 2003	1:24,000
7.5-minute quadrangle of Squaxin Island; .pdf	Logan et al., 2003	1:24,000
7.5-minute quadrangle of Tumwater; .pdf	Walsh et al., 2003	1:24,000
2014 ESRI ArcGIS geodatabase for Geology of Washington State	DGER	1:24,000

Table 4: Fields in the attribute table for the DOGAMI protocol

The twenty-four data fields used in the landslide geodatabase as outlined in the DOGAMI protocol (Burns and Madin, 2009).

Field Name	Brief Description	Field Name	Brief Description
QUADNAME	7.5 minute quadrangle name	FAIL_DEPTH	Failure depth, estimated and/or calculated slope normal thickness of failure depth
UNIQUE_ID	"QUADNAME"_"ID"; ex. Shelton_1	FAN_HEIGHT	Change in elevation from top to toe of fan
TYPE_MOVE	Type of movement from	FAN_DEPTH	Estimated and/or calculated fan depth
MOVE_CLASS	Movement Classification Name	DEEP_SHAL	Deep (>4.5m or 15ft) or shallow seated
MOVE_CODE	Movement Classification Code	HS_IS1	Horizontal distance from head scarp to internal scarp no.1
CONFIDENCE	Confidence of identification	IS1_IS2	Horizontal distance from internal scarp no.1 to internal scarp no.2
AGE	Estimated age	IS2_IS3	Horizontal distance from internal scarp no.2 to internal scarp no.3
DATE_MOVE	Date of last known movement	IS4_IS5	Horizontal distance from internal scarp no.4 to internal scarp no.5
NAME	Landslide name	HD_AVE	Calculation of average horizontal distance between internal scarps
GEOL	Geologic unit	DIRECT	Direction of movement using azimuth in increment of 22.5°
SLOPE	Adjacent slope angle	AREA	Area of landslide deposit
HS_HEIGHT	Head scarp height: Change in elevation from bottom to top of head scarp	VOLUME	Volume of landslide deposit

Table 5: List of landslides and complexes identified in this study

Landslides mapped for this study using the DOGAMI protocol. The landslide's unique ID is a combination of the 7.5-minute quadrangle title and the order the landslide was mapped. Landslides with an alphanumeric combination do not fit with the DOGAMI standard for creating a unique name, but during my iterations, I needed a way to keep picture and well log files together, but distinguish separate movements.

#	Landslide's Unique ID & Name	Area, including scarp (ft^2)	Area, including scarp (m^2)
1	Summit_Lake_1a	423,020	39,300
2	Summit_Lake_1c	101,340	9,420
3	Summit_Lake_1b	125,990	11,710
4	Summit Lake_2	152,000	14,120
5	Summit Lake_3a	1,890	180
6	Summit Lake_3b	2,640	250
7	Summit Lake_3c	9,530	890
8	Summit Lake_4	89,310	8,300
9	Shelton_1	172,740	16,050
10	Shelton_2a	3,710	350
11	Shelton_2b	7,900	734
12	Shelton_3a	5,710	530
13	Shelton_3b	3,090	290
14	Shelton_4	234,050	21,740
15	Shelton_5	940,620	87,390
16	Squaxin Island_1	247,320	22,980
17	Squaxin Island_1b	16,880	1,570
18	Squaxin Island_2	545,050	50,640
19	Squaxin Island_3	36,610	3,400
20	Squaxin Island_4pt1	55,420	5,150
21	Squaxin Island_4pt2	918,660	85,350
22	Squaxin Island_5	64,740	6,020
23	Squaxin Island_6/ Carlyon Beach/Hunter Point Road	1,977,780	183,740
24	Squaxin Island_7	960,230	89,210
25	Squaxin Island_8	285,280	26,500
26	Squaxin Island_9	91,670	8,520
27	Squaxin Island_10	106,320	9,880
28	Squaxin Island_11	152,270	14,150
29	Squaxin Island_12	164,750	15,310
30	Squaxin Island_13	103,540	9,620
31	Squaxin Island_14	102,800	9,550
32	Tumwater_1	227,950	21,180
33	Tumwater_2	1,470	140
34	Tumwater_3	5,930	550
35	Tumwater_4/ Sunrise Beach (within Tumwater_5)	474,070	44,040
36	Tumwater_5*	1,128,950	104,880
	Total Area (counting Tumwater_4/Sunrise only once because it is a reactivation within Tumwater_5)	**9,467,160 ft^2**	**879,530 m^2**

Table 6: Classification of landslides and the types of movements along Steamboat Island Peninsula

The 19 classifications modified from Varnes and Cruden (1996) and used in the DOGAMI protocol (Burns and Madin, 2009).

Type of Movement	Type of Material		
	Rock	**Debris**	**Soil**
Fall	**RF** rock fall	**DF** debris fall	**EF** earth fall
Topple	**RT** rock topple	**DT** debris topple	**ET** earth topple
Slide-rotational	**RS-R** rock slide - rotational	**DS-R** debris slide - rotational	**ES-R** earth slide - rotational
Slide-translational	**RS-T** rock slide - translational	**DS-T** debris slide - translational	**ES-T** earth slide - translational
Lateral Spread	**RSP** rock spread	**DSP** debris spread	**ESP** earth spread
Flow	**RFL** rock flow	**DFL** debris flow	**EFL** earth flow
Complex	**C** complex or combinations of two or more types		

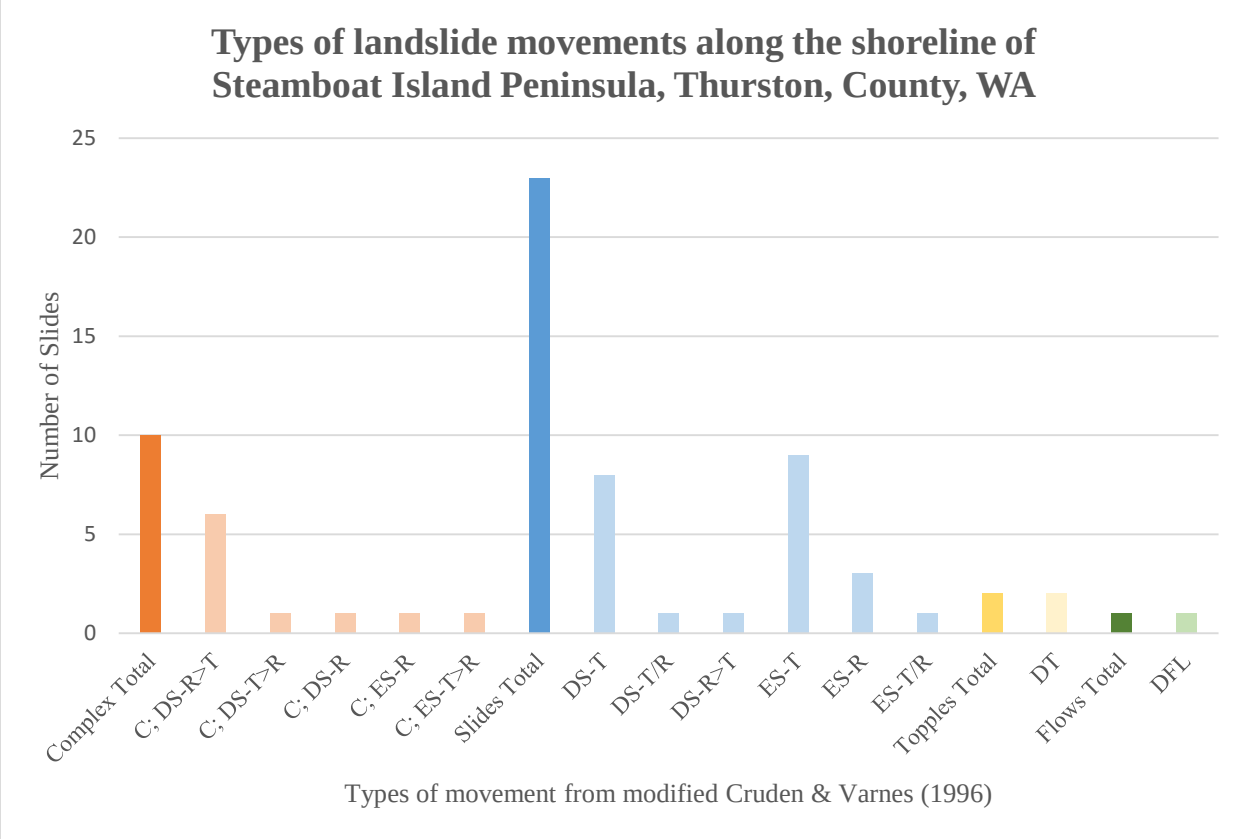

Table 7: Types of movement for the 36 landslide deposits

The 36 landslide deposits mapped for this study, showing the type of movement, movement classification, and movement code, which come from the DOGAMI protocol listed in Table 6 (Burns and Madin, 2009).

Unique ID for landslide	Type of Movement	Movement Classification	Movement abreviation
Shelton_1	Slide	Debris Slide - Translational	DS-T
Shelton_2a	Slide	Earth Slide - Translational	ES-T
Shelton_2b	Slide	Earth Slide - Translational	ES-T
Shelton_3a	Slide	Debris Slide - Translational	DS-T
Shelton_3b	Slide	Debris Slide - Translational	DS-T
Shelton_4	Complex	Debris Slide - Rotational & Translational	C; DS-R>T
Shelton_5	Complex	Complex Debris Slide--Rotational	C; DS-R
Squaxin Island_1	Complex	Complex Debris Slide - Rotational & Translational	C; DS-R>T
Squaxin Island_1b	Slide	Debris Slide - Translational	DS-T
Squaxin Island_2	Complex	Complex Debris Slide - Rotational & Translational	C; DS-R>T
Squaxin Island_3	Slide	Earth Slide - Translational	ES-T
Squaxin Island_4pt1	Slide	Debris Slide - Translational	DS-T
Squaxin Island_4pt2	Slide	Debris Slide - Translational>Rotational	DS-T>R
Squaxin Island_5	Slide	Debris Slide - Translational	ES-T
Squaxin Island_6	Complex	Complex Earth Slide - Rotational	C; ES-T>R
Squaxin Island_7	Slide	Earth Slide - Rotational	ES-R
Squaxin Island_8	Slide	Earth Slide - Rotational	ES-R
Squaxin Island_9	Slide	Earth Slide - Translational	ES-T
Squaxin Island_10	Slide	Earth Slide - Translational	ES-T
Squaxin Island_11	Slide	Earth Slide - Rotational - Translational	ES-T; ES-R
Squaxin Island_12	Slide	Earth Slide - Translational	ES-T
Squaxin Island_13	Slide	Earth Slide - Translational	ES-T
Squaxin Island_14	Slide	Earth Slide - Translational; Topple	ES-T; ET
Summit_Lake_1a	Complex	Complex Debris Slide--Rotation & Translation	C
Summit_Lake_1b	Complex	Complex Debris Slide--Rotation & Translation	C
Summit_Lake_1c	Complex	Complex Debris Slide--Rotation & Translation	C
Summit Lake_2	Complex	Complex Debris Slide--Translational & Rotational	C; DS-T>R
Summit Lake_3a	Slide	Debris Slide - Translational	DS-T
Summit Lake_3b	Slide	Debris Slide - Translational	DS-T
Summit Lake_3c	Slide	Debris Slide - Translational	DS-T
Summit Lake_4	Topple	Debris Topple	DT
Tumwater_1	Slide	Debris Slide - Rotational>Translational	DS-R>T
Tumwater_2	Topple	Debris Topple	DT
Tumwater_3	Flow	Debris Flow	DFL
Tumwater_4	Slide	Earth Slide - Rotational	ES-R
Tumwater_5	Complex	Complex Earth Slide - Rotational	C; ES-R

Table 8: Ages of landslides on Steamboat Island Peninsula

Landslide ages based on aerial photos, orthorectified NAIP imagery, and oblique aerial photos taken by the Washington Department of Ecology.

Unique ID for landslide	AGE	Date of Movements
Squaxin Island_8	Historic	Prior to 1977
Tumwater_5*	Historic	Prior to 1965
Summit_Lake_1a	Historic & Modern	Prior to 1965; prior to 2000; prior to 2006
Summit_Lake_1b	Historic & Modern	Prior to 1965; prior to 2000; prior to 2006
Summit_Lake_1c	Historic & Modern	Prior to 1965; prior to 2000; prior to 2006
Shelton_4	Historic & Modern	Prior to 1965; prior to 2000; prior to 2006
Shelton_5	Historic & Modern	Prior to 1965; prior to 2006
Squaxin Island_1	Historic & Modern	Prior to 1965; Prior to 2000; Prior to 2006
Squaxin Island_2	Historic & Modern	Prior 1977; prior to 2000; prior to 2006
Squaxin Island_4pt2	Historic & Modern	Prior to 1977; prior 2000; prior 2006
Squaxin Island_6/ Carlyon Beach	Historic & Modern	Prior 1977;1996-97; 2/6/1999- 5/1999; 2001, 2006-07
Squaxin Island_7	Historic & Modern	Prior to 1977; prior 2000; prior 2006
Squaxin Island_11	Historic & Modern	Prior to 1977?, visible in 2000
Tumwater_1	Historic & Modern	Prior to 1977; Prior to 2000
Tumwater_4/ Sunrise Beach	Historic & Modern	Documented movement in 1999; 2001 (inclinometers)
Summit Lake_2	Modern	Prior to 1965; between 1977 to 2000; prior 2006
Summit Lake_3a	Modern	Prior to 2000
Summit Lake_3b	Modern	Between 2000 and 2006
Summit Lake_3c	Modern	Prior to 2000
Summit Lake_4	Modern	Prior 1977; prior 2000; prior 2006
Shelton_1	Modern	Prior to 1977; prior to 2000
Shelton_2a	Modern	Prior to 1977; prior to 2000; prior to 2006
Shelton_2b	Modern	Prior to 1977; prior to 2000; prior to 2006
Shelton_3a	Modern	Prior to 1977
Shelton_3b	Modern	Between 2011-2013 (NAIP)
Squaxin Island_1b	Modern	Prior to 2006
Squaxin Island_3	Modern	Prior to 1977; prior to 2006
Squaxin Island_4pt1	Modern	Prior to 1977; prior 2000; prior 2006
Squaxin Island_5	Modern	Prior to 1977; prior to 2006
Squaxin Island_9	Modern	Prior to 1977; Between 2000 and 2006
Squaxin Island_10	Modern	Prior to 1977; Between 2000 and 2006
Squaxin Island_12	Modern	Prior to 1977; prior to 2000
Squaxin Island_13	Modern	Prior to 1977; prior to 2006
Squaxin Island_14	Modern	Prior to 1977; between 2000 & 2006
Tumwater_2	Modern	Between 2000 and 2006
Tumwater_3	Modern	Prior to 1977

Table 9: Depth and slope angle of Steamboat Island Peninsula landslides

The landslides mapped in this study and ordered from lowest to steepest slope. Deep landslides have a lower slope, while shallow landslides have a steeper slope.

Unique ID for landslide	Deep or Shallow landslide (based on 4.5m or 15ft)	SLOPE in °
Squaxin Island_6 (Carlyon Beach)	Deep	10
Squaxin Island_8	Deep	10
Squaxin Island_7	Deep	11
Squaxin Island_2	Deep	12
Squaxin Island_5	Shallow	12
Tumwater_5*	Deep	13
Squaxin Island_1b	Shallow	14
Squaxin Island_11	Deep	14
Shelton_5	Deep	15
Squaxin Island_1	Deep	15
Squaxin Island_3	Deep	16
Squaxin Island_12	Deep	16
Summit_Lake_1a	Deep	18
Summit_Lake_1b	Deep	18
Summit_Lake_1c	Deep	18
Shelton_1	Deep	20
Tumwater_1	Deep	20
Shelton_4	Deep	21
Squaxin Island_9	Shallow	22
Squaxin Island_14	Deep	25
Squaxin Island_4pt1	Shallow	26
Squaxin Island_13	Deep	26
Summit Lake_2	Deep	27
Squaxin Island_4pt2	Shallow	29
Tumwater_3	Shallow	29
Tumwater_4 (Sunrise Beach)	Deep	30
Shelton_2a	Shallow	31
Summit Lake_3b	Shallow	32
Summit Lake_3a	Shallow	33
Squaxin Island_10	Shallow	33
Shelton_2b	Shallow	34
Shelton_3a	Shallow	34
Shelton_3b	Shallow	34
Tumwater_2	Shallow	34
Summit Lake_3c	Shallow	36
Summit Lake_4	Deep	Topple

Table 10: Direction of landslide movement

Landslide movement based on a sixteen-spoke compass rose. The majority of the landslides move towards the northwest or east-southeast.

Unique Landslide ID	DIRECTION
Summit_Lake_1c	0
Summit_Lake_1b	0
Summit Lake_3a	0
Tumwater_2	0
Squaxin Island_6/ Carlyon Beach	22.5
Squaxin Island_1	90
Squaxin Island_8	90
Squaxin Island_1b	90
Tumwater_1	90
Squaxin Island_7	90
Squaxin Island_5	90
Squaxin Island_13	90
Tumwater_4/ Sunrise Beach	112.5
Squaxin Island_11	112.5
Tumwater_5	112.5
Squaxin Island_12	112.5
Squaxin Island_14	112.5
Squaxin Island_9	135
Squaxin Island_10	135
Tumwater_3	180
Shelton_3b	225
Shelton_3a	225
Shelton_4	270
Shelton_2a	270
Shelton_2b	270
Shelton_5	315
Shelton_1	315
Summit Lake_4	315
Squaxin Island_4pt1	315
Squaxin Island_4pt2	315
Summit Lake_3b	315
Summit Lake_2	337.5
Summit_Lake_1a	337.5
Squaxin Island_2	337.5
Squaxin Island_3	337.5
Summit Lake_3c	337.5

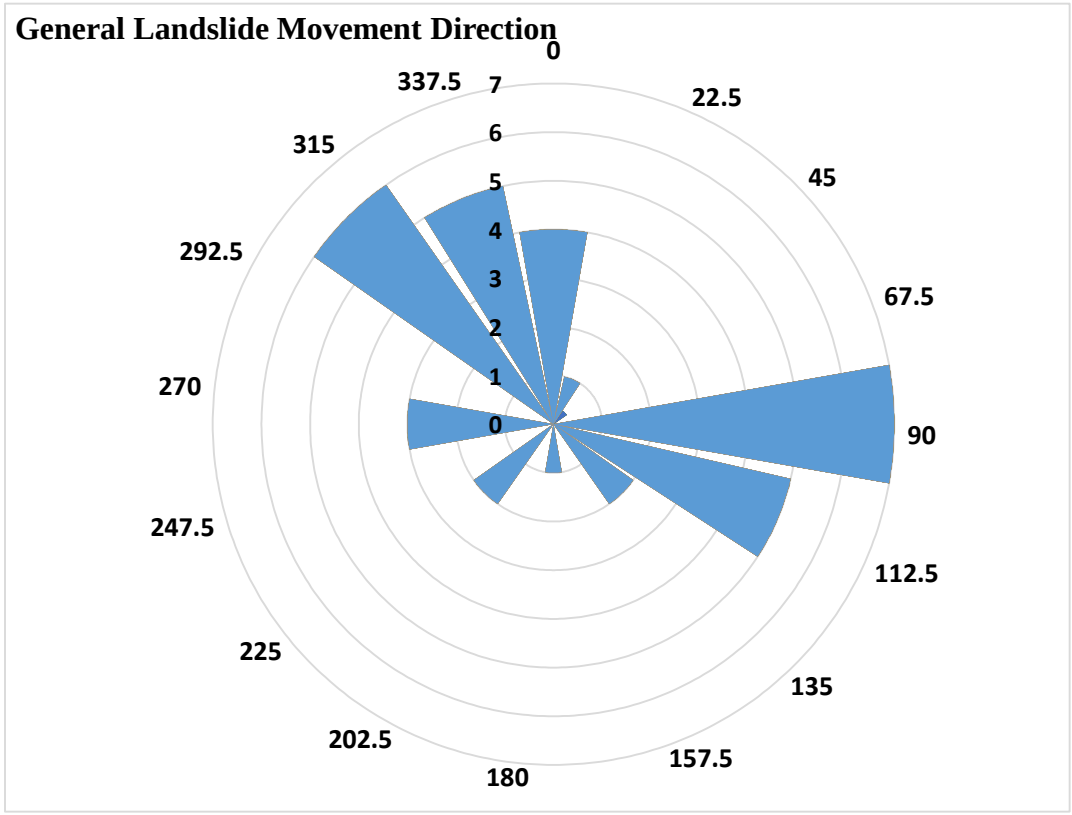

Table 11: Reasons for not mapping landslides that the DGER (2009) study includes

Landslides from the DGER (2009) inventory of Steamboat Island Peninsula that I did not identify in this study. The 'Slide ID' refers to the landslide from the DGER study, and the 'DML Evaluation' is the reason I did not recognize the landslide or map the area as a landslide deposit.

Slide_ID	Total in Category	DML_Evaluation
40	2	Bathymetry needed; all underwater
521		Bathymetry needed; all underwater
510	1	Bathymetry needed; Did not see this landslide due to modification
452	4	Disagree: Shape doesn't fit the ridge
449		Disagree: Shape doesn't fit the ridge
501		Disagree; Features unclear in lidar
39		Disagree; I don't see these features on lidar
4	2	Doesn't align with features on lidar
5		Doesn't align with features on lidar
6	9	Fluvial; Doesn't align with lidar
47		Fluvial; How is it separated from the landslide below?
70		Fluvial; I would not have mapped as a ls
520		Fluvial; I would not have mapped this large of a ls; I have Squazin_Island_8 within
67		Fluvial; I would not have mapped this ls
518		Fluvial; I would not have mapped this ls
68		Fluvial; I would not have picked out as ls
69		Fluvial; I would not have picked out as ls
261		Fluvial; Looked fluvial to me
71	3	I would not have mapped as a ls
547		Inconsistent; Not sure why this would get mapped, but not the similar features N of this location
3		No lidar coverage
48	3	Small; hummocks
50		Small; hummocks
49		Small; must reflect something in photo
546	4	Steep shoreline with hummocks; I wasn't sure if fluvial or not
548		Steep shoreline with hummocks; I wasn't sure if fluvial or not
225		Steep shoreline with hummocks; I wasn't sure if fluvial or not
226		Steep shoreline with hummocks; I wasn't sure if fluvial or not
503	7	Too modified
512		Too modified
513		Too modified
514		Too modified
529		Too modified
515		Too modified; where is end of fluvial and beginning ls
568		Too modified; within cove

Table 12: Trends in certainty and landslide identification

Trends between the landslide certainty as defined by the DGER (2009) and the landslides mapped in this study (DML Findings).

Certainty (defined by DGER, 2009)	# of slides DGER (2009) findings & area covered	DML Findings	Percentage of area in common
1 = Definite	123; covers area of 658,160 m^2 (12,740,500 ft^2)	80 = Agree 40 = Understand; steep slope 3 = other	56%
2 = Probable	58; covers area of 489,120 m^2 (5,187,330 ft^2)	24 = Agree 30 = Understand; steep slope 4 = other	30%
3 = Questionable; data complier is not certain, but including for completeness	55; covers area of 2,093,860 m^2 (22,538,150 ft^2)	6 = Agree 25 = Understand; steep slope 3 = Disagree 2 = Bathymetry needed (under water) 8 = Fluvial 5 = Too modified	5%
4 = Prior account, but not verified in this report	20; covers area of 40,870 m^2 (439,890 ft^2)	8 = Agree 9 = Understand; steep slope 1 = Disagree 2 = Fluvial	64%
5 = Prior account; verified	8; covers area of 16,380 m^2 (176,330 ft^2)	5 = Agree 3 = Understand; steep slope	40%

Table 13: Comparison of this study to the DGER (2009) - area impacted by landslides

The DGER (2009) mapped 159 landslide complexes on Steamboat Island Peninsula; however, several of these landslides were not directly verified by DGER but instead came from previous works. The area covered by these landslides and the toes of landslides that reach beneath the Puget Sound and require bathymetry are subtracted from this total area. This shows that the DOGAMI protocol, while office based rather than field based, can accurately map landslides.

Description	DGER (2009)	This Study
Total Area of landslide coverage	3,256,570 m^2 (35,053,400 ft^2)	879,530 m^2 (9,467,160 ft^2)
- Questionable Area	2,093,860 m^2 (22,538,150 ft^2)	NA
- Area within toe requiring bathymetry	289,760 m^2 (3,118,930 ft^2)	NA
Total Landslide Area mapped with Certainty	872,950 m^2 (9,396,320 ft^2)	879,530 m^2 (9,467,160 ft^2)

Table 14: Comparison of landslide classifications

Comparison of the landslides identified using the twelve DGER (2009) classifications of movement versus the classification from the DOGAMI protocol, which are based on Cruden and Varnes (1996).

Landslide Type according to DGER (2009)	# of study slides with portion of ID similar / # DGER Identified slides in category	DML_Evaluation
None indicated	7 / 8	3 x Squaxin_Island_7 (Deep - Rotational) 3 x Squaxin_Island_7 (Deep - Rotational); Bathymetry extends into depth 1 x Squaxin_Island_4pt2 (Shallow - Debris Slide – Translational> Rotational)
1 = Shallow undifferentiated	7 / 22	7 x Squaxin_Island_4pt2 (**Shallow** - Debris Slide – Translational> Rotational) 2 x Part of Summit_Lake_2 (Deep - Complex; Translational & Rotational) 1 x Shelton _1 (Deep - Debris Slide – Translational) 1 x Bottom half is in Summit Lake_4 (Debris Topple)
2 = Debris Flow – includes debris avalanche & "shallow colluvium" (Shannon & Wilson, 2000)	9 / 15	1 x Squaxin_Island_4pt1 (**Shallow** - **Debris** Slide – Translational) 6 x Squaxin_Island_4pt2 (**Shallow** - **Debris** Slide – Translational> Rotational) 1 x Part of Summit Lake_2 (Deep - Complex; Translational & Rotational) 2 x Part of Squaxin_Island_3 (Deep - **Earth** Slide – Translational)
3 = Debris Slide	8	1 x Part of Squaxin_Island_7 (Deep – Earth Slide - Rotational) 2 x Squaxin_Island_4pt2 (Shallow - **Debris** Slide – Translational> Rotational)
4 = "Groundwater blowout" (Shannon & Wilson, 2000)	0 / 4	1 x Part of Shelton_1 (Deep – Debris Slide – Translational) 1 x Part of Squaxin_Island_9 (Shallow – Earth Slide – Translational)
5 = Block fall or topple – includes fall/ topple of rock/debris/earth material, and "high bluff peel-off" of Shannon & Wilson (2000)	35 / 86	1 x Shelton_2a (**Shallow** – **Earth** Slide – Translational) 1 x Shelton_2b (**Shallow** – **Earth** Slide – Translational) 1 x Part of Summit_Lake_2 (Deep - Complex; Translational & Rotational) 5 x Part of Summit_Lake_4 (**Debris Topple**) 1 x Portion of Tumwater_2 (**Debris Topple**) 1 x Portion of **scarp** of Squaxin_Island_1 (Deep – Complex **Debris** Slide – Rotational & Translational) 2 x Squaxin_Island_2 (Deep – Complex **Debris** Slide - Translational & Rotational) 2 x Part of Squaxin_Island_4pt1 (**Shallow** - **Debris** Slide – Translational) 11 x Part of Squaxin_Island_4pt2 (**Shallow** - **Debris** Slide – Translational> Rotational) 3 x Part of Squaxin_Island_9 (**Shallow** – **Earth** Slide – Translational) 5 x Part of Squaxin_Island_10 (**Shallow** – **Earth** Slide – Translational) 1 x Part of Squaxin_Island_12 (Deep – **Earth** Slide – Translational) 2 X Part of Squaxin_Island_14 (Deep– **Earth** Slide – Translational; **Topple**)
6 = Deep-seated Undifferentiated	17 / 44	1 x Part of Squaxin_Island_1 scarp (**Deep** - **Complex** Debris Slide - Rotational & Translational) 2 x Part of Squaxin_Island_2 (**Deep** – **Complex** Debris Slide - Translational & Rotational) 2 x Part of Squaxin_Island_4pt2 (Shallow - Debris Slide – Translational> Rotational) 1 x Within Squaxin Island_6 (**Deep** - **Complex** Earth Slide – Rotational)

		1 x Squaxin_Island_8 (**Deep** - Earth Slide – Rotational) 2 x Squaxin_Island_11 (**Deep** - Earth Slide - Rotational – Translational) 2 x Squaxin_Island_12 (**Deep** – Earth Slide – Translational) 2 x Part of Squaxin_Island_13 (**Deep** - Earth Slide – Translational) 2 x Squaxin_Island_14 (**Deep**– Earth Slide – Translational; Topple) 1 x Summit_Lake_2 (**Deep** - **Complex** Debris Slide--Translational & Rotational) 3 x Tumwater_1 (**Deep** - Debris Slide - Rotational>Translational)
7 = Deep-seated - earthflow	0 / 3	I did not map any landslides in this area
8 = Deep-seated – translational	2 / 4	1 x Part of Squaxin_Island_4pt2 (Shallow - Debris Slide – **Translational**> Rotational) 1 x Squazin_Island_8 within (**Deep** - Earth Slide – Rotational)
9 = Deep-seated - rotational	6 / 15	1 x Summit Lake_1b (**Deep** - Complex Debris Slide--**Rotational** & Translation) 1 x Summit Lake_1c (**Deep** - Complex Debris Slide--**Rotational** & Translation) 1 x Summit Lake_3a within (Shallow Debris Slide – Translational) 1 x Squaxin Island_1 (**Deep** - Complex Debris Slide - **Rotational** & Translational) 1 x Squaxin Island_2 (**Deep** - Complex Debris Slide - **Rotational** & Translational) 1 x Squaxin Island_9 (Shallow - Earth Slide – Translational) 1 x Tumwater_4 / Sunrise Beach Landslide (**Deep** - Earth Slide – **Rotational**) 1 x Tumwater_5 (**Deep** - Complex Earth Slide – **Rotational**)
10 = Deep-seated - composite	4 / 6	1 x Summit Lake_1a within (**Deep** - **Complex** Debris Slide--**Rotation & Translation**) 1 x Squaxin Island_6 Carlyon Beach/Hunter Point Landslide (**Deep** - **Complex** Earth Slide – Rotational) 1 x Shelton_4 (**Deep** - **Complex** Debris Slide - **Rotational & Translational**) 1 x Shelton_5 (**Deep** - **Complex** Debris Slide—Rotational)
11 = Undifferentiated / unknown	19 / 47	1 x Shelton_1 (Deep - Debris Slide – Translational) 2 x Shelton_4 (Deep - Complex Debris Slide - Rotational & Translational) 1 x Squaxin Island_2 (but not entire swath) (Deep - Complex Debris Slide - Rotational & Translational) 3 x Squaxin Island_4pt2 (Shallow - Debris Slide - Translational>Rotational) 3 x Shoreline of Squaxin Island_6 Carlyon Beach/ Hunter Point (I didn't map separately) 2 x Squaxin Island_11 (Deep - Earth Slide - Rotational – Translational) 3 x Squaxin Island_12 (Deep - Earth Slide - Rotational – Translational) 1 x Summit Lake_1 (Deep - Complex Debris Slide--Rotation & Translation) 1 x Overlap with Summit Lake_3c (Shallow - Debris Slide – Translational) 1 x Tumwater 1 (Deep - Debris Slide - Rotational>Translational) 1 x Tumwater 5 (Deep - Complex Earth Slide – Rotational)
12 = other	2 / 2	1 x Squaxin Island 4pt2 (Shallow - Debris Slide - Translational>Rotational) 1 x Squaxin_Island_5 (Shallow - Debris Slide – Translational)

Table 15: Hungr et al. (2004) proposed update to Varnes classification system

Proposed update to the Varnes classification system, which uses six general types of movement and bases material on geotechnical terms (table adapted from Hungr et al., 2014).

Type of movement	Rock	Soil
Fall	Rock/ice fall	Boulder/debris/silt fall
Topple	Rock block topple	Gravel/sand/silt topple
	Rock flexural topple	
Slide	Rock rotational slide	Clay/silt rotational slide
	Rock planar slide	Clay/silt planar slide
	Rock wedge slide	Gravel/sand/debris slide
	Rock compound slide	Clay/silt compound slide
	Rock irregular slide	
Spread	Rock slope spread	Sand/silt liquefaction spread
		Sensitive clay spread
Flow	Rock/ice avalanche	Sand/silt/debris dry flow
		Sand/silt/debris flowslide
		Sensitive clay flowslide
		Debris flow
		Mud flow
		Debris flood
		Debris avalanche
		Earthflow (retained for previous research)
		Peat flow
Slope Deformation	Mountain slope deformation	Soil slope deformation
	Rock slope deformation	Soil creep
		Solifluction

Appendix A : Confidence scores and geology sources for landslides

Name of landslide	Head Scarp	Flanks	Toe	Internal	Total Points	Geology source: Well logs, Geologic Maps, Technical Reports
Summit_Lake_1	5	5	1	0	11	Ashey; Chambers; Reeves
Summit_Lake_2	6	6	1	0	13	None
Summit_Lake_3a	7	6	2	0	15	DeBoer; Merchant
Summit_Lake_3b	6	6	2	0	14	Merchant
Summit_Lake_3c	5	5	1	0	11	Merchant
Summit_Lake_4	9	4	2	0	15	Hackett
Shelton_1	8	4	1	0	13	Patek
Shelton_2	6	5	1	0	12	Dekker
Shelton_3a	6	5	1	0	12	Stratigraphy: Shelton 13
Shelton_3b	5	5	1	0	11	Stratigraphy: Shelton 13
Shelton_4	7	5	1	5	18	Stratigraphy: Shelton 12
Shelton_5	7	4	1	6	18	Shelton Geologic Map; Stevens well log w/out address
Squaxin_Island_1	6	5	1	0	12	Nord; Geologic Map
Squaxin_Island_2	8	5	1	0	14	Stenchever
Squaxin_Island_3	6	5	1	0	12	Calder; Geologic Map
Squaxin_Island_4	8	5	1	0	14	Fountaine; Geologic Map
Squaxin_Island_5	8	6	1	0	15	Geologic Map
Squaxin_Island_6	9	8	1	7	25	GeoEngineers Report 1999
Squaxin_Island_7	8	7	1	5	21	Hall
Squaxin_Island_8	8	6	1	5	20	Similar to Hall
Squaxin_Island_9	8	6	1	0	15	James; Geologic Map
Squaxin_Island_10	8	6	1	0	15	James; Geologic Map
Squaxin_Island_11	7	4	1	0	12	Dye; Geologic Map

Squaxin_Island_12	7	6	1	0	14	Funderbirk; Geologic Map
Squaxin_Island_13	8	5	1	0	14	Funderbirk; Taylor
Squaxin_Island_14	7	5	1	0	13	Funderbirk; Taylor
Tumwater_1	6	5	1	0	12	Midles
Tumwater_2	7	5	1	0	13	Eaton; Geologic Map
Tumwater_4	9	9	1	8	27	Shannon & Wilson Report; Geologic Map